An Iterative Technique for Instrument Transformer Calibration and Line Parameter Estimation with Synchrophasor Measurements

Yvonne Agnes Pearl Tauro

Thesis submitted to the faculty of the Virginia Polytechnic Institute and State University
in partial fulfillment of the requirements for the degree of

Master of Science
In
Electrical Engineering

Virgilio A. Centeno, Chair
Arun G. Phadke, Co-Chair
James S. Thorp
Jaime De La Reelopez

February 15, 2017
Blacksburg, VA

Keywords: Synchrophasor measurements, Instrument Transformer, Calibration, Transmission Line Parameters, Estimation, Kalman Filter

An Iterative Technique for Instrument Transformer Calibration and Line Parameter Estimation with Synchrophasor Measurements

Yvonne Agnes Pearl Tauro

Abstract

The introduction of synchrophasor technology to the realm of power systems has presented a myriad of novel approaches to age-old problems. In this thesis, the questions of instrument transformer calibration and transmission line parameter estimation have been examined. With synchrophasors offering real-time data for analysis, a solution to each individual problem seems feasible. A quandary however arises due to the fact that calibration methods depend on accurate knowledge of line parameters, and estimation of these parameters depend on calibrated measurements. Traditional methods of determining the parameters may not be the most accurate due to a variety of fluctuations possible on the system, which is why real-time estimation could prove beneficial. This work analyzes each problem and a feasible solution and proposes a method to achieve transducer calibration as well as parameter estimation together, while employing synchronized phasor measurements.

An Iterative Technique for Instrument Transformer Calibration and Line Parameter Estimation with Synchrophasor Measurements

Yvonne Agnes Pearl Tauro

General Audience Abstract

Synchrophasor Measurement Units (PMUs) provide the magnitude and angle of the quantity being measured, along with GPS time synchronization. Voltage, current and frequency data can be sent to a central control centre at the rate of 30 or 60 times per second. With a sufficient number of PMUs deployed on the electric grid, system operators now have available essentially a 'snapshot' of the system, which aids to monitor the grid, predict abnormal conditions as well as quickly identify troubled areas and accordingly take remedial actions.

In order to facilitate the safe and reliable operation of the electric power grid, there are numerous devices that monitor quantities such as voltage, current, frequency etc. Most of these devices however are incapable of handling high levels of voltage and currents that are common to the power network. Instrument transformers (IT) are used to step down the measured quantities to much lower magnitudes that can then be analyzed by downstream devices. Each instrument transformer has a specified transformation ratio. For example, a voltage transformer with a transformation ratio of 100:1 would step down 500V to 5V. With time, these ITs may experience wear which might lead to degradation of its ratio, which would in turn be detrimental for applications relying on accurate measurements. Therefore routine calibration of ITs is desired. Traditional methods of calibration however involve taking the device out of service temporarily. As one can imagine, this is cost, labour and time intensive. With the availability of PMU data, it is now possible to perform calibration of these devices without having to take the device offline, provided we have accurate knowledge of the transmission line parameters.

The parameters of a transmission line include the resistance, reactance and susceptance of the line and depend on the type of conductor used, the length and ambient temperature. Therefore seasonal and daily temperature variations can cause changes in the line parameters. With PMU data, we now have the capability to estimate these parameters, so that we have the most accurate idea of the present parameters. However for this, calibrated voltages and currents are required.

Herein we face a quandary: we need to calibrate the ITs, which require accurate line parameters, but to estimate the current line parameters we need calibrated voltages and currents. This is the problem this thesis addresses. First, methods to perform both tasks, i.e. instrument transformer calibration as well as line parameter estimation using PMU measurements are analyzed. Finally an iterative method is proposed that can be applied to solve both problems together.

Acknowledgements

I would like to express my sincere gratitude to Dr. Centeno, for his continuous guidance and invaluable support throughout my time at Virginia Tech. I have been indeed lucky to have such a patient and encouraging mentor. To Dr. Phadke and Dr. Thorp for constantly advising me through research, and for always making time to quell my doubts. My thanks to Dr. De La Reelopez as well, for being a wonderful teacher and for serving on my committee. It has truly been a privilege to have learned from all of you. Finally, my utmost thanks to my parents and brother. I am blessed to have such a supportive family. Thank you all.

Contents

List of Figures

List of Tables

Chapter 1: Synchrophasors and their Applications

1.1.1 The Age of the Synchrophasor

The phase angles on the power grid have long been of concern to power engineers. It is an established fact that the real power flow of a line is directly proportional to the sine of the voltage angle difference at either end of the line. Therefore there have been several attempts to accurately capture this difference, with some early experiments conducted in the 80s [1-3]. These methods involved the measurement of phase angle at each bus by observing the next positive going zero crossing of a single phase voltage waveform and then comparing them to a common time reference. However these methods had certain limitations, in the fact that they could not be applicable for large systems, and that they used time references that were not universal. Harmonics present on the waveforms were also not considered.

Improvement in computing capacity also allowed for the implementation of more efficient algorithms, involving the positive sequence voltage of a network. The work [4] developed a method to measure the phase angle and frequency of the system without relying on the zero crossing detection. This work has been referred to as the starting point of modern synchrophasor technology [5]. The first prototypes of the 'Phasor Measurement Unit' (PMU) were built at Virginia Tech in the early 80s leading to the manufacturing of the first commercial unit by Macrodyne in 1992 [6]. Today there are several manufacturers of PMUs, with the demand for deploying these devices on the network growing across the world.

1.1.2 Synchrophasor Concepts

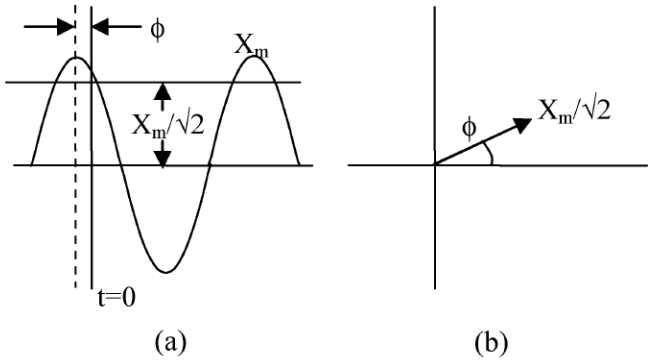

Figure 1.1: A Waveform in (a) Sinusoidal representation and (b) Phasor representation [7]

Let us consider a pure sinusoidal waveform such as

$$x(t) = X_m \cos(wt + \varphi) \tag{1.1}$$

This can be expressed in terms of a phasor, given by

$$X \equiv \frac{X_m}{\sqrt{2}} \varepsilon^{j\theta} = \frac{X_m}{\sqrt{2}} \ (cos\varphi + jsin\varphi) \tag{1.2}$$

X_m is the peak value of the waveform, w is the frequency and φ is the phase angle.

While the above expressions represent a static waveform, in reality we need to deal with constantly changing waveforms, which is why PMUs view the input signal over a finite window of time for computing the phasor. Usually this is a multiple of the time period of the fundamental frequency of the signal, which for most power application is 50/60 Hz. The PMU uses data samples taken over the window to compute the Discrete Fourier Transform (DFT). For example, if $x_0, x_1, x_2, \ldots\ldots, x_{N-1}$ are the N samples collected, the phasor computed with the DFT is given by [5]

$$X = \frac{\sqrt{2}}{N} \sum_{k=0}^{N-1} x_k \varepsilon^{-jk\left(\frac{2\pi}{N}\right)}$$

(1.3)

PMUs are also equipped with frequency tracking, which adjusts the sampling window accordingly. This is beneficial in times when signals deviate from nominal frequency. The DFT ensures that harmonics are eliminated. Anti-aliasing filters are also incorporated. Time synchronism is achieved via a GPS signal. A sampling clock within the PMU locks onto the one pulse per second signal from GPS satellites, thus providing an accurate time reference. This enables time-tagging of the phasors. Quantities form different locations can now be aligned according to their time stamp, providing an overall picture of the system behavior.

1.1.3 Applications of PMUs

Today synchronized phasor measurement units are employed for an increasing number of applications. Most of these functions aim towards the monitoring, protection and control of the grid, with the end goal being to avoid calamitous failures, or to at least reduce the severity in unavoidable cases.

Some of the earliest PMUs deployed were used to study manually triggered events [7]. At the time there were certain limitations like communication bandwidth. Today with dedicated, secure communications paths PMUs can provide real-time system awareness at the operation centers directly. Several utilities have also developed in house tools for data visualization. Post mortem analysis of system events can also be conducted more efficiently, due to the time stamped nature of synchrophasor data.

Frequency, which is a key indicator of the health of the system, is another quantity that is easily available through synchrophasor data. Generation loss directly shows in the frequency of the system, and can lead to a travelling electromechanical wave. An event

like this is what lead to the development of the Frequency Monitoring Network (FNET) [8]. Monitoring frequency data facilitates early detection of power oscillations, and can be used to predict generation loss, islanding and increase in tie-line separation.

State estimation is another application that has benefited through PMU technology. Traditionally, line power flows and used to compute the voltages at the buses, which form the states of the system. However, when scanning a wide-area system for this data, certain time elapses between observing two points in the system. Thus a potential time lag would be assumed. This was overcome by assuming that the system was static during the time of the scan. Depending on how long the scan would take, the states formed might differ from what the actual system states were. With PMUs being able to report up to 60 times per second, the time skew problem is greatly reduced. It is now possible to observe the power system dynamically.

Protection and control systems also stand to gain from synchrophasor measurements. PMU data allows for efficient implementation of adaptive protection methods that can study the system before taking a decision through voting schemes. Power system control is traditionally local, relying on feedback. The introduction of PMUs enables monitoring and control of remote quantities. Discrete switching controls can now be provided remotely via synchrophasors [9]. Local control means are thereby improved when operated with both local and remote inputs.

Synchrophasor data is also critical for offline analytics. Power system planning and dynamic models are maintained by utilities to ensure minimal power outages and optimal economic dispatch. With the availability of synchrophasor data of normal and abnormal operation points, system model data and simulations can be compared and validated.

The importance of base-lining studies has gained importance in recent years. System PMU data from different operating points, load profiles, temperatures and other conditions can be studied to understand how the phase angle behaves. The phase angle

directly relates to the stress on the system. Therefore the operating limits of the network can be determined and alarms set accordingly.

In addition to the functions mentioned above, there is plenty of utility for synchronized phasor data. The calibration of instrument transducers has been an old persistent problem, but one that can certainly be improved with phasor measurements. Methods of transmission line parameter estimation with PMU measurements will also be discussed in the following sections. The reason why these two applications are highlighted here is because each has a direct influence on the other. An error present on either one would lead to errors while determining the other. In the subsequent chapters, methods for both transformer calibration and line parameter estimation will be developed. Finally, an iterative method that assumes both the transducers as well as the line parameters have errors will be used to arrive at the calibrated values and estimates of the line parameters.

1.2 Contemporary methods of Transformer Calibration

Theoretically, the calibration of current transformers (CTs) and voltage transformers (VTs) should not be a complicated task; the ratio and angle correction factors need to be determined for different values of excitation at the primary winding and different levels of loading on the secondary [10]. This can be done by comparing the output of the device under test to the output of a standard transformer, while both have the same transformation ratios and are excited by the same signal. Usually an instrument called the transformer comparator (TC) is used to achieve this. The comparator's operation is based generally on the concepts developed by Kusters and Moore [11]. Most of the TCs today are automated and referred to as measurements transformer test set (MTTS).

A new current comparator and voltage transformer calibrator was built at the Technical University of Budapest, as described by [12]. This instrument employed built-in programmable analog signal processors that enabled self-calibration and calibration of voltage transformers of different ratios with increased speed and accuracy measurements.

The method proposed in the article [13] proposed a simple and novel structure for an MTTS. Requiring simple hardware of moderate complexity and cost, the method achieved measurement uncertainties that were within the acceptable range at the time. The article [14] built upon this method, by implementing digital signal processing of the secondary signals of the two transformers, thereby reducing cost and improving accuracy.

In the article [15] an original method of voltage and current transformer calibration was introduced that made use of optical fiber sensor technology. The high precision optical transducers could be installed simultaneously with conventional CTs and VTs to avoid interruption of power supply, therefore making the method an on-line calibration. Optic fiber transducers are certainly known for their accuracy, but also tend to be extremely expensive, which is why a utility might choose to use only a very small number of them.

The paper [16] presented a method of calibrating CTs and PTs using synchrophasor measurements in the positive sequence domain. The proposed method also outlined a method for optimal placement of calibrated devices on a power network, in order to reduce the errors of all measurements. The methods proposed in the works [17] and [18] also use phasor measurements to calibrate instrument transformers, considering a three phase network. These methods will be discussed in more detail in the next chapter.

1.3 Contemporary methods of Transmission Line Parameter Estimation

Accurate knowledge of transmission line parameters is highly desired as it results in increased accuracy of relay settings, impedance-based fault location as well as power flow modelling. Traditionally, computer programs are used to calculate the line parameters, based on conductor dimensions, tower geometries, engineer estimates of line lengths, etc. This process however could have some inaccuracies introduced due to sag computation, which is dependent on temperature. In addition, the ambient temperature of the line as well as the loading effects also alter the line parameters. The introduction of

synchrophasor technology presents a benefits the process by allowing the parameters to be estimated in real-time based on current conditions and flows.

The paper [19] develops an approach to estimate the line parameters from historical data. Simulated data from a power system model is used, as well as SCADA data. An interesting concept discussed here is how the errors present in planning models can affect the line parameters' estimates and how synchrophasor measurements used to estimate them can also help validate the system model. The paper proposes means to deal with the uncertainty and errors present when dealing with real SCADA data.

One of the first papers to use synchrophasor measurements to estimate line parameters was [20]. The work presented here used PMU data collected during a decommissioning test to estimate the ABCD parameters of the line. A particular set of events were used for this. The ABCD parameters were also calculated using traditional methods (software, EMTP). Finally the power flows from the measurements were compared to the power flows calculated by using the estimated ABCD parameters (with a different set of events). The measured and computed power flows were found to be very close, therefore validating the method.

The work [21] compared four methods, two classical and two proposed ones to estimate the line parameters of a short transmission line. Phasor measurements simulated through ATP were used for this. Among the methods described, the authors found the multiple measurement method using linear regression to work best.

For short lines that have PMU measurements available from only one end, the article [22] proposed a new method. The methodology estimated parameters using PMU measurements from one end, and states from a hybrid state estimator from the other end. The hybrid state estimator uses both conventional and synchrophasor data. While the method worked well on the small test system, it made an assumption that only one line's parameters were erroneous.

An algorithm for estimating the parameters of a line or transformer was proposed in the article [23]. The method used a weighted least squares estimation on a test system using a number of measurement sets. A moving window of data sets was used, thereby allowing for parameters to be estimated in real-time, including parameters that might change due to certain events (series compensation, tap changing). There was however a stringent assumption of PMUs available at either end of the element.

1.4 Scope of Work

In addition to the functions mentioned above, there is plenty of utility for synchronized phasor data. The calibration of instrument transducers has been an old persistent problem, but one that can certainly be improved with phasor measurements. In Chapter 2 one method of transducer calibration is discussed in detail. Chapter 3 examines a method of transmission line parameter estimation. The reason why these two applications are highlighted here is because each has a direct influence on the other. An error present on either one would lead to errors while determining the other. In the subsequent chapters, methods for both transformer calibration and line parameter estimation will be developed. Finally, in Chapter 4 an iterative method will be developed to arrive at the calibrated values and estimates of the line parameters. This method operates under the assumption that both sets of data, i.e. the voltage and current measurements as well as line parameter data has errors present.

Chapter 2: Instrument Transformer Calibration

2.1 Background

Instrument transformers are widely used at different points on the electric power grid, mainly to provide voltages and currents that are more easily handled by downstream devices, such as relays, control devices and synchrophasors. Typically, the stepped down voltages are around 120V (line to line), and currents are 5A, but this can vary according to region (in Europe, secondary currents are 1A). In addition, instrument transformers help isolate the sensitive measuring devices from the high voltage primary network.

Instrument transformers can be classified into voltage and current transformers, based on what signal they measure. Current transformers are slightly different from voltage transformers because of the fact that their primary winding is connected in series with the power circuit. Therefore these are sometimes called 'series transformers'. Voltage transformers are connected in parallel to the power circuit, and can be broadly split into two groups: inductive voltage and the capacitor voltage transformers (CVT). CVTs may be used for high voltage levels (145kV and up) while inductive voltage transformers are more economical and are used for lower voltage levels[24].

There are different standards set for accuracy ratings according to the International Electrotechnical Commission (IEC) and the Institute of Electrical and Electronics Engineers (IEEE). The instrument transformers are classified into metering class (M class) and protection class (P class) according to these IEC and IEEE standards[10]. The protection class devices are mainly used for relaying applications. Metering class equipment are used for revenue purposes, for example on tie lines, or at nodes in the system where higher accuracy is desired, and these devices are held to more stringent accuracy requirements. These are usually more expensive than the protection class devices. Most relays, synchrophasors and SCADA devices get their signals from P class devices.

With new highly accurate metering devices for monitoring and control systems relying on instrument transformers for their inputs, the introduced by the instrument transformers cannot be ignored. These errors could creep in due to age, usage, operating conditions, environmental or other factors. The IEEE standard defines the Ratio Correction Factor (RCF) of an instrument transformer as the ratio between the actual transformation ratio to the nameplate ratio of the device. This translates to the ratio between the actual measured value, and what value is actually expected as per the nameplate details. The RCF consists of the magnitude correction factor, which should ideally be in the range of 3-10%, and the phase angle correction factor (ACF), which should be in the range of 2-6.7 degrees. For an ideal transformer, the ratio correction factor should be 1, and the phase angle correction factor 0.

Utilities can perform calibration of these transformers to ensure that their errors are within reasonable limits. However on-site calibration tends to be time consuming and expensive in terms of money and labor. References [18] and [17] develop a method to automatically calibrate these transformers based on PMU measurements. This method could be run twice a day or as required depending on load profile. In addition, this method doesn't require the transformer to be temporarily taken out of service, which should make it more appealing for utilities. It requires only one voltage transformer to be 'perfect', i.e. calibrated previously.

It should be noted that the final value at the output of the synchrophasor has an error that has two contributors: the measuring transformer error, and the PMU error itself. The method mentioned above assumes that the PMU error is separate from the instrument transformer error, and the calibration is performed assuming that the error seen in the measured values are errors from the instrument transformer alone. That is, only instrument transformer calibration is performed, assuming PMUs to be already calibrated for minimal error.

2.2 The Two Bus Model

2.2.1 Calibrating the Two Bus System

To understand the method developed in [17], let us consider the two bus system as per the figure below:

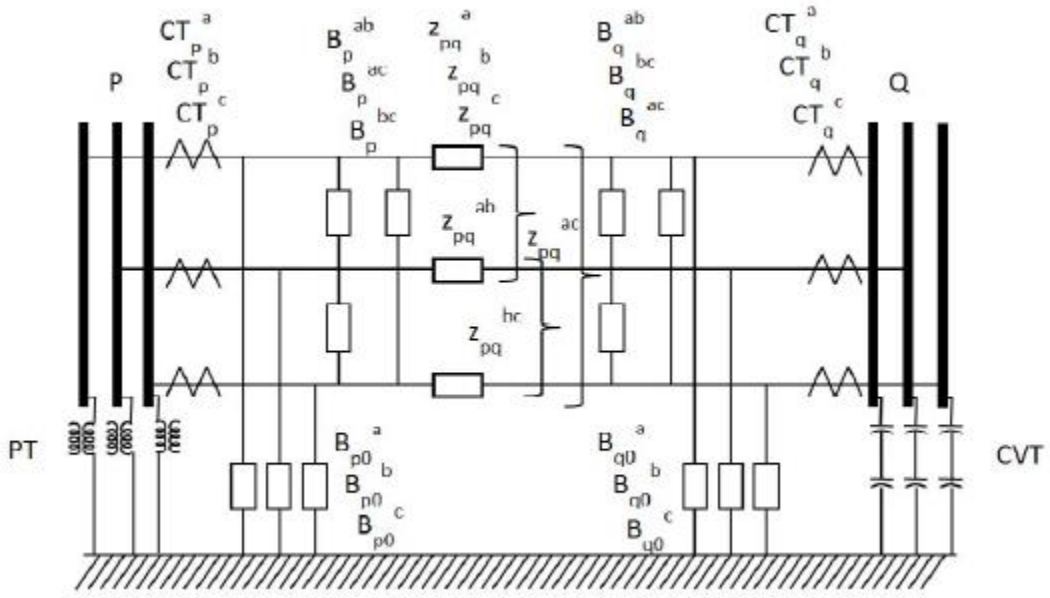

Figure 2.1: A two bus, three phase system

Figure 2.1 describes two buses, 'P' and 'Q' connected via a three phase pi-model transmission line. The line has its three phase impedance described by,

$$Z_{pq}^{abc} = \begin{bmatrix} Z_{pq}^{a} & Z_{pq}^{ab} & Z_{pq}^{ac} \\ Z_{pq}^{ab} & Z_{pq}^{b} & Z_{pq}^{bc} \\ Z_{pq}^{ac} & Z_{pq}^{bc} & Z_{pq}^{c} \end{bmatrix} \tag{2.1}$$

And line admittance by,

$$Y_{pq}^{abc} = (Z_{pq}^{abc})^{-1} = \begin{bmatrix} Y_{pq}^{a} & Y_{pq}^{ab} & Y_{pq}^{ac} \\ Y_{pq}^{ab} & Y_{pq}^{b} & Y_{pq}^{bc} \\ Y_{pq}^{ac} & Y_{pq}^{bc} & Y_{pq}^{c} \end{bmatrix} \tag{2.2}$$

The susceptance value at either ends of the line can be described by

$$B_{p0}^{abc} = j\begin{bmatrix} B_{p0}^{a} + B_{p0}^{ab} + B_{p0}^{ac} & -B_{p0}^{ab} & -B_{p0}^{ac} \\ -B_{p0}^{ab} & B_{p0}^{b} + B_{p0}^{ba} + B_{p0}^{bc} & -B_{p0}^{bc} \\ -B_{p0}^{ac} & -B_{p0}^{bc} & B_{p0}^{c} + B_{p0}^{ca} + B_{p0}^{cb} \end{bmatrix} \quad (2.3)$$

$$B_{q0}^{abc} = j\begin{bmatrix} B_{q}^{a} + B_{q0}^{ab} + B_{q}^{ac} & -B_{q0}^{ab} & -B_{q0}^{ac} \\ -B_{q0}^{ab} & B_{q0}^{b} + B_{q0}^{ba} + B_{q0}^{bc} & -B_{q0}^{bc} \\ -B_{q0}^{ac} & -B_{q0}^{bc} & B_{q0}^{c} + B_{q0}^{ca} + B_{q0}^{cb} \end{bmatrix} \quad (2.4)$$

The p, q subscripts refer to bus index, a, b, c subscripts refer to phase index, and 0 refers to ground.

Let us assume that both buses ‘P’ and ‘Q’ have three phase voltage and current transformers connected at each terminal of the transmission line. Let the voltage transformer at ‘P’ be an ideal transformer, therefore having magnitude ratio correction factor as 1 and phase angle correction factor 0.

Assuming no extraneous losses and applying Ohm’s law, we can obtain:

$$V_q^{abc} = V_p^{abc} - Z_{pq}^{abc}(I_{pq}^{abc} - B_{p0}^{abc} * V_p^{abc}) \quad (2.5)$$

$$V_p^{abc} = V_q^{abc} - Z_{pq}^{abc}(I_{qp}^{abc} - B_{q0}^{abc} * V_q^{abc}) \quad (2.6)$$

where V_p^{abc} : three phase voltage at ‘P’

V_q^{abc} : three phase voltage at ‘Q’

I_{pq}^{abc} : three phase currents flowing from ‘P’ to ‘Q’

I_{qp}^{abc} : three phase currents flowing from ‘Q’ to ‘P’

Now the error model for a PMU can be given by the following equation [17]:

$$X^{abc} = diag(K_m^{abc}) * X_m^{abc} \quad (2.7)$$

Where X^{abc} : the true value of the measured signal, as seen at the input of the PMU

X_m^{abc} : the measured value of the signal, as output of the PMU

K_m^{abc}: the ratio correction factor

It should be noted that the ratio correction factor employed here is the inverse of the conventional correction factor, i.e. K_m^{abc} here is the ratio of the input to the output. This has been done to simplify further calculations involving K_m^{abc}.

Based on equation (2.7), the relations of voltages and currents of the synchrophasor can be written as:

$$V_0^{abc} = diag(K_v^{abc})V^{abc} \quad (2.8)$$

$$I_0^{abc} = diag\left(K_i^{abc}\right)I^{abc} \quad (2.9)$$

Where V_0^{abc}: true value of three phase voltage vector

V^{abc}: measured value of voltage vector

K_v^{abc}: three phase correction factor of the voltage transformer

I_0^{abc}: true value of three phase current vector

I^{abc} : measured value of current vector

K_i^{abc}: three phase correction factor of current transformer

Using the above relations in equations (2.5) and (2.6), we get:

$$diag(K_{vq}^{abc})V_q^{abc} = diag(K_{vp}^{abc})V_p^{abc} - Z_{pq}^{abc}(diag\left(K_{ipq}^{abc}\right)I_{pq}^{abc} - B_{p0}^{abc}\ diag(K_{vp}^{abc})V_p^{abc}) \quad (2.10)$$

$$diag(K_{vp}^{abc})V_p^{abc} = diag(K_{vq}^{abc})V_q^{abc} - Z_{pq}^{abc}(diag(K_{iqp}^{abc})I_{qp}^{abc} - B_{q0}^{abc}diag\left(K_{vq}^{abc}\right)V_q^{abc}) \quad (2.11)$$

Our objective is to determine the values of the correction factors from the above equations. We know the values of voltages and currents. Let us assume at this stage that the line parameters accurately represent the line. Considering the three phase form of the equations, we have six equations and nine unknowns. K_{vp}^{abc} is 1+0j for each phase, as we assume that the voltage transformer at 'P' is perfect. This is an underdetermined set of equations, i.e. we do not have sufficient information to accurately calculate the remaining correction factors. To overcome this, measurements under different loading scenarios are considered. This results in 6*n number of equations, where n is the number of loading conditions considered.

$$\left.\begin{aligned}
diag\left(K_{vq}^{abc}\right)V_{q1}^{abc} &= diag\left(K_{vp}^{abc}\right)V_{p1}^{abc} - Z_{pq}^{abc}\left(diag\left(K_{ipq}^{abc}\right)I_{pq1}^{abc} - B_{p0}^{abc}\, diag\left(K_{vp}^{abc}\right)V_{p1}^{abc}\right)\\
diag\left(K_{vp}^{abc}\right)V_{p1}^{abc} &= diag\left(K_{vq}^{abc}\right)V_{q1}^{abc} - Z_{pq}^{abc}\left(diag\left(K_{iqp}^{abc}\right)I_{qp1}^{abc} - B_{q0}^{abc} diag\left(K_{vq}^{abc}\right)V_{q1}^{abc}\right)\\
diag\left(K_{vq}^{abc}\right)V_{q2}^{abc} &= diag\left(K_{vp}^{abc}\right)V_{p2}^{abc} - Z_{pq}^{abc}\left(diag\left(K_{ipq}^{abc}\right)I_{pq2}^{abc} - B_{p0}^{abc}\, diag\left(K_{vp}^{abc}\right)V_{p2}^{abc}\right)\\
diag\left(K_{vp}^{abc}\right)V_{p2}^{abc} &= diag\left(K_{vq}^{abc}\right)V_{q2}^{abc} - Z_{pq}^{abc}\left(diag\left(K_{iqp}^{abc}\right)I_{qp2}^{abc} - B_{q0}^{abc} diag\left(K_{vq}^{abc}\right)V_{q2}^{abc}\right)\\
&\vdots\\
diag\left(K_{vq}^{abc}\right)V_{qn}^{abc} &= diag\left(K_{vp}^{abc}\right)V_{pn}^{abc} - Z_{pq}^{abc}\left(diag\left(K_{ipq}^{abc}\right)I_{pqn}^{abc} - B_{p0}^{abc}\, diag\left(K_{vp}^{abc}\right)V_{pn}^{abc}\right)\\
diag\left(K_{vp}^{abc}\right)V_{pn}^{abc} &= diag\left(K_{vq}^{abc}\right)V_{qn}^{abc} - Z_{pq}^{abc}\left(diag\left(K_{iqp}^{abc}\right)I_{qpn}^{abc} - B_{q0}^{abc} diag\left(K_{vq}^{abc}\right)V_{qn}^{abc}\right)
\end{aligned}\right\} \quad (2.12)$$

1, 2…..n represent the load scenarios.

By appropriately choosing 'n', we can estimate the correction factors. With some rearranging, the equations of (2.12) can be written as:

$$\left.\begin{aligned}
diag\left(K_{vp}^{abc}\right)Y_{pq}^{abc}V_{p1}^{abc} &= diag\left(K_{vq}^{abc}\right)\left(Y_{pq}^{abc} + B_{q0}^{abc}\right)V_{q1}^{abc} - diag\left(K_{iqp}^{abc}\right)I_{qp1}^{abc}\\
diag\left(K_{vp}^{abc}\right)\left(Y_{pq}^{abc} + B_{p0}^{abc}\right)V_{p1}^{abc} &= diag\left(K_{vq}^{abc}\right)Y_{pq}^{abc}V_{q1}^{abc} + diag\left(K_{ipq}^{abc}\right)I_{pq1}^{abc}\\
diag\left(K_{vp}^{abc}\right)Y_{pq}^{abc}V_{p2}^{abc} &= diag\left(K_{vq}^{abc}\right)\left(Y_{pq}^{abc} + B_{q0}^{abc}\right)V_{q2}^{abc} - diag\left(K_{iqp}^{abc}\right)I_{qp2}^{abc}\\
diag\left(K_{vp}^{abc}\right)\left(Y_{pq}^{abc} + B_{p0}^{abc}\right)V_{p2}^{abc} &= diag\left(K_{vq}^{abc}\right)Y_{pq}^{abc}V_{q2}^{abc} + diag\left(K_{ipq}^{abc}\right)I_{pq2}^{abc}\\
&\vdots\\
diag\left(K_{vp}^{abc}\right)Y_{pq}^{abc}V_{pn}^{abc} &= diag\left(K_{vq}^{abc}\right)\left(Y_{pq}^{abc} + B_{q0}^{abc}\right)V_{qn}^{abc} - diag\left(K_{iqp}^{abc}\right)I_{qpn}^{abc}\\
diag\left(K_{vp}^{abc}\right)\left(Y_{pq}^{abc} + B_{p0}^{abc}\right)V_{pn}^{abc} &= diag\left(K_{vq}^{abc}\right)Y_{pq}^{abc}V_{qn}^{abc} + diag\left(K_{ipq}^{abc}\right)I_{pqn}^{abc}
\end{aligned}\right\}$$

(2.13)

In matrix form,

$$\begin{bmatrix} Y_{pq}^{abc}V_{p1}^{abc} \\ \left(Y_{pq}^{abc}+B_{p0}^{abc}\right)V_{p1}^{abc} \\ Y_{pq}^{abc}V_{p2}^{abc} \\ \left(Y_{pq}^{abc}+B_{p0}^{abc}\right)V_{p2}^{abc} \\ . \\ . \\ . \\ Y_{pq}^{abc}V_{pn}^{abc} \\ \left(Y_{pq}^{abc}+B_{p0}^{abc}\right)V_{pn}^{abc} \end{bmatrix} = \begin{bmatrix} \left(Y_{pq}^{abc}+B_{q0}^{abc}\right)diag(V_{q1}^{abc}) & zero(3,3) & -diag(I_{qp1}^{abc}) \\ Y_{pq}^{abc}diag(V_{q1}^{abc}) & diag(I_{pq1}^{abc}) & zero(3,3) \\ \left(Y_{pq}^{abc}+B_{q0}^{abc}\right)diag(V_{q2}^{abc}) & zero(3,3) & -diag(I_{qp1}^{abc}) \\ Y_{pq}^{abc}diag(V_{q2}^{abc}) & diag(I_{pq2}^{abc}) & zero(3,3) \\ . & . & . \\ . & . & . \\ . & . & . \\ \left(Y_{pq}^{abc}+B_{q0}^{abc}\right)diag(V_{qn}^{abc}) & zero(3,3) & -diag(I_{qp1}^{abc}) \\ Y_{pq}^{abc}diag(V_{qn}^{abc}) & diag(I_{pq1}^{abc}) & zero(3,3) \end{bmatrix} \begin{bmatrix} K_{vq}^{abc} \\ K_{ipq}^{abc} \\ K_{iqp}^{abc} \end{bmatrix}$$

(2.14)

In the above equation, the unknowns that we wish to find are in the matrix containing K_{vq}^{abc}, K_{ipq}^{abc}, K_{iqp}^{abc}. These are the correction factors for the voltage transformer at 'Q' and current transformers at either end of the line. This matrix should be of dimensions 9 x 1. The other matrix on the right hand side should have dimensions 6n x 9, where n is the number of load scenarios. The matrix on the left hand side should have dimensions 6n x 1. Now we can estimate our unknowns using least squares estimation, which has been described in [5]. This method requires the equations to be in a linear form such as:

$$y = Ax \tag{2.15}$$

where y is the set of measurements, x is the set of unknown states and A has more rows than columns. The proper form of this equation would be:

$$y = Ax + \varepsilon \tag{2.16}$$

where ε represents the error in measurements. The optimization problem is to find the estimate, $\hat{x}$ which minimizes

$$E\{(y - A\hat{x})^T(y - A\hat{x})\} = y^T y - 2y^T A\hat{x} - \hat{x}^T A^T A\hat{x} \tag{2.17}$$

The optimum solution is

$$\hat{x} = (A^T A)^{-1} A^T y \tag{2.18}$$

with the error given by

$$error = y - A\hat{x} \tag{2.19}$$

2.2.2 Applying the method

To get an idea of how the method works, let us consider a transmission line between two buses. Simulations were performed in PSS/E for different load conditions to obtain voltage and current values. The original voltages and currents are given in the following tables.

Vp					
Phase A		Phase B		Phase C	
Mag. (p.u.)	Angle (deg)	Mag. (p.u.)	Angle (deg)	Mag. (p.u.)	Angle (deg)
1.036786	-76.8839	0.999207	158.4886	1.000976	38.40214
1.036767	-77.5741	1.001862	157.5099	1.004683	37.81086
1.036747	-78.2654	0.998558	157.5426	0.996437	36.95764
1.036728	-78.9576	1.002246	156.907	1.000208	36.27691
1.036708	-79.6509	1.002569	156.1491	1.003674	36.28013
1.036688	-80.3453	0.998797	154.9046	1.002128	35.16756
1.036668	-81.0452	1.004281	154.7411	1.004234	34.41093
1.036649	-81.7495	1.00513	154.1942	1.003167	33.80699
1.036629	-82.451	1.001868	153.008	0.998523	32.6916
1.036608	-83.1588	0.999017	152.7798	1.003092	32.18009

Table 2.1: Voltages at bus ‘P’ for different load conditions

Vq					
Phase A		Phase B		Phase C	
Mag. (p.u.)	Angle (deg)	Mag. (p.u.)	Angle (deg)	Mag. (p.u.)	Angle (deg)
1.043398	-71.1366	1.002827	164.557	1.011099	44.59972
1.043366	-71.8232	1.008211	164.0836	1.00178	43.54911
1.043334	-72.5109	1.008168	162.6246	1.002234	43.15552
1.043302	-73.1995	1.004758	162.4818	1.006957	42.54807
1.04327	-73.8892	1.004834	161.5589	1.004787	41.70697
1.043238	-74.58	1.010491	161.0352	1.009455	41.35857
1.043206	-75.2764	1.00328	160.313	1.010347	39.82265
1.043173	-75.9771	1.010574	159.4851	1.002149	39.88883
1.04314	-76.6749	1.008094	159.127	1.010592	39.16946
1.043106	-77.3792	1.003135	158.6022	1.006803	38.32971

Table 2.2: Voltages at bus ‘Q’ for different load conditions

Ipq					
Phase A		Phase B		Phase C	
Mag. (p.u.)	Angle (deg)	Mag. (p.u.)	Angle (deg)	Mag. (p.u.)	Angle (deg)
15.46925	99.80787	14.8686	-22.522	14.97324	-138.982
15.99586	102.063	15.40778	-24.0506	14.11798	-135.558
15.52853	96.43204	13.11045	-27.4379	14.48122	-137.234
15.43353	96.98678	13.92578	-24.124	14.986	-138.748
15.27686	98.3017	13.27903	-26.3081	13.40563	-136.513
15.904	96.33056	15.06569	-29.0061	14.75642	-141.707
15.03127	97.04302	13.68297	-26.4023	13.52542	-140.618
15.68323	94.58491	13.24454	-28.4591	14.49973	-137.821
15.66273	93.59116	15.1655	-28.6207	15.44769	-145.373
15.64385	93.7715	14.26594	-28.7093	14.8011	-142.124

Table 2.3: Currents as observed from bus ‘P’

Iqp					
Phase A		Phase B		Phase C	
Mag. (p.u.)	Angle (deg)	Mag. (p.u.)	Angle (deg)	Mag. (p.u.)	Angle (deg)
15.421	-75.35	14.898	162.18	14.908	45.71
16.012	-73.26	15.419	160.5	14.146	49.397
15.433	-78.75	13.073	157.92	14.485	47.585
15.367	-78.16	13.964	160.9	14.97	45.931
15.257	-76.79	13.291	158.97	13.453	48.707
15.853	-78.95	15.031	155.65	14.704	43.055
15.016	-77.98	13.72	158.72	13.524	44.58
15.624	-80.64	13.254	156.85	14.561	46.994
15.598	-81.63	15.181	156.01	15.363	39.168
15.599	-81.44	14.291	156.19	14.803	42.617

Table 2.4: Currents as observed from bus ‘Q’

To these values, errors were applied to simulate measurements obtained at the output of the PMU. These errors were of the order of 10e-2 for magnitude and 0.05 degrees for the angle. Subsequently, the calibration method was applied in order to obtain the true values. The voltages at ‘P’ are assumed to be ‘perfect’ i.e. without error, hence these values have a correction factor of 1, therefore the pre and post calibration values are equal. The post calibration values of voltages at ‘Q’ and currents as seen from either end are given below.

Vq Post Calibration Values					
Phase A		Phase B		Phase C	
Mag. (p.u.)	Angle (deg)	Mag. (p.u.)	Angle (deg)	Mag. (p.u.)	Angle (deg)
1.0434	-71.14	1.0029	164.56	1.011	44.602
1.0434	-71.83	1.0083	164.09	1.0017	43.551
1.0433	-72.52	1.0082	162.63	1.0022	43.157
1.0433	-73.21	1.0048	162.49	1.0069	42.55
1.0433	-73.9	1.0049	161.56	1.0047	41.709
1.0432	-74.59	1.0106	161.04	1.0094	41.36
1.0432	-75.28	1.0033	160.32	1.0103	39.825
1.0432	-75.98	1.0106	159.49	1.0021	39.891
1.0431	-76.68	1.0082	159.13	1.0105	39.171
1.0431	-77.39	1.0032	158.61	1.0067	38.332

Table 2.5: Post Calibration voltages at bus ‘Q’

Ipq Post Calibration Values					
Phase A		Phase B		Phase C	
Mag. (p.u.)	Angle (deg)	Mag. (p.u.)	Angle (deg)	Mag. (p.u.)	Angle (deg)
15.457	101	14.88	-21.29	14.978	-137.8
15.984	103.26	15.42	-22.82	14.123	-134.3
15.517	97.628	13.121	-26.21	14.486	-136
15.422	98.182	13.937	-22.9	14.991	-137.5
15.265	99.497	13.289	-25.08	13.41	-135.3
15.892	97.526	15.077	-27.78	14.761	-140.5
15.02	98.239	13.694	-25.17	13.53	-139.4
15.671	95.78	13.255	-27.23	14.504	-136.6
15.651	94.787	15.177	-27.39	15.453	-144.2
15.632	94.967	14.277	-27.48	14.806	-140.9

Table 2.6: Post Calibration currents as observed from bus ‘P’

Iqp Post Calibration Values					
Phase A		Phase B		Phase C	
Mag. (p.u.)	Angle (deg)	Mag. (p.u.)	Angle (deg)	Mag. (p.u.)	Angle (deg)
15.432	-76.56	14.904	160.95	14.917	44.506
16.023	-74.47	15.425	159.27	14.155	48.192
15.444	-79.96	13.078	156.68	14.494	46.38
15.378	-79.37	13.97	159.67	14.98	44.726
15.267	-78	13.296	157.74	13.462	47.503
15.864	-80.16	15.037	154.42	14.713	41.85
15.026	-79.19	13.725	157.48	13.533	43.375
15.634	-81.85	13.259	155.62	14.57	45.789
15.608	-82.84	15.187	154.77	15.373	37.964
15.61	-82.65	14.297	154.96	14.812	41.413

Table 2.7: Post Calibration currents as observed from bus ‘Q’

The difference in the original values and the values estimated or the corrected values by the algorithm are in the range of 10e-4 for voltages. For currents this difference is larger, with a maximum deviation of about 0.3 p.u. With the inclusion of an accurate current measurement, it would be possible to obtain a better estimate of the actual currents, and thereby the correction factors of the CTs. This would require an update of the equations previously described, to account for an RCF of 1 for the perfect CT.

Since at this point we know the errors that are applied to the true values of voltages and currents, we can also compute the errors in estimation of the correction factors.

Errors in PT CF		
	Mag. (p.u.)	**Ang. (deg.)**
Phase A	-3.10E-06	0.0069
Phase B	-6.73E-05	-0.004
Phase C	7.60E-05	-0.002

Table 2.8: Errors in Correction Factors of the Voltage Transformer

Errors in CT CF				
	Ipq		**Iqp**	
	Mag. (p.u.)	Ang. (deg.)	Mag. (p.u.)	Ang. (deg.)
Phase A	0.0007	-1.196	-7E-04	1.2105
Phase B	-7E-04	-1.229	-4E-04	1.2323
Phase C	-3E-04	-1.21	-9E-04	1.2045

Table 2.9: Errors in Correction Factors of the Current Transformers

2.3 Calibration on a Multi-Bus System

2.3.1 Propagating the Calibration Method

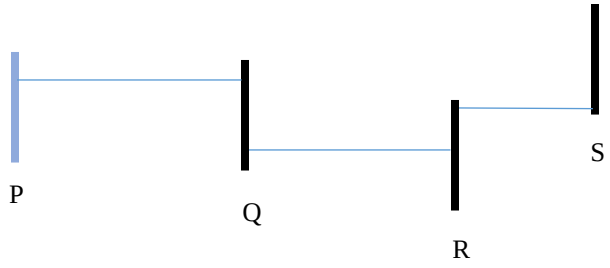

Figure 2.2: A Four Bus Network

Consider a section of a slightly larger network, as shown above. The presumption here is that all the lines are equipped with synchrophasors at both ends. Ideally, synchrophasor

measurements would be available at each bus of a system. Cost and labor constraints may cause a hindrance to this however, which is why utilities often choose to deploy PMUs in stages, providing different levels of observability at each stage, until complete observability is attained [25]. For the network in figure 2.2, let us assume that the ideal voltage transformer is at bus 'P'. We can use this measurement to calibrate buses further away so long as they have a connected path to 'P', either directly or via other buses.

We know the relation for the buses 'P' and 'Q':

$$\begin{bmatrix} Y_{pq}^{abc}V_{p1}^{abc} \\ \left(Y_{pq}^{abc}+B_{p0}^{abc}\right)V_{p1}^{abc} \\ . \\ . \\ . \\ Y_{pq}^{abc}V_{pn}^{abc} \\ \left(Y_{pq}^{abc}+B_{p0}^{abc}\right)V_{pn}^{abc} \end{bmatrix} = \begin{bmatrix} \left(Y_{pq}^{abc}+B_{q0}^{abc}\right)diag(V_{q1}^{abc}) & zero(3,3) & -diag(I_{qp1}^{abc}) \\ Y_{pq}^{abc}diag(V_{q1}^{abc}) & diag(I_{pq1}^{abc}) & zero(3,3) \\ . & . & . \\ . & . & . \\ . & . & . \\ \left(Y_{pq}^{abc}+B_{q0}^{abc}\right)diag(V_{qn}^{abc}) & zero(3,3) & -diag(I_{qp1}^{abc}) \\ Y_{pq}^{abc}diag(V_{qn}^{abc}) & diag(I_{pq1}^{abc}) & zero(3,3) \end{bmatrix} \begin{bmatrix} K_{vq}^{abc} \\ K_{ipq}^{abc} \\ K_{iqp}^{abc} \end{bmatrix} \tag{2.20}$$

This gives us the correction factors for voltage at bus 'Q' and for currents measured at either end of the line. Since we need to calibrate all voltage and current transformers, for buses 'Q' and 'R' the equations would be slightly different, as shown below:

$$\begin{bmatrix} zero(3,1) \\ zero(3,1) \\ . \\ . \\ . \\ zero(3,1) \\ zero(3,1) \end{bmatrix} = \begin{bmatrix} -Y_{qr}^{abc}V_{q1}^{abc} & \left(Y_{qr}^{abc}+B_{r0}^{abc}\right)diag(V_{r1}^{abc}) & zero(3,3) & -diag(I_{rq1}^{abc}) \\ -\left(Y_{qr}^{abc}+B_{q0}^{abc}\right)V_{q1}^{abc} & Y_{qr}^{abc}diag(V_{r1}^{abc}) & diag(I_{qr1}^{abc}) & zero(3,3) \\ . & . & . & . \\ . & . & . & . \\ . & . & . & . \\ -Y_{qr}^{abc}V_{qn}^{abc} & \left(Y_{qr}^{abc}+B_{r0}^{abc}\right)diag(V_{rn}^{abc}) & zero(3,3) & -diag(I_{rq1}^{abc}) \\ -\left(Y_{qr}^{abc}+B_{q0}^{abc}\right)V_{qn}^{abc} & Y_{qr}^{abc}diag(V_{rn}^{abc}) & diag(I_{qr1}^{abc}) & zero(3,3) \end{bmatrix} \begin{bmatrix} K_{vq}^{abc} \\ K_{vr}^{abc} \\ K_{iqr}^{abc} \\ K_{irq}^{abc} \end{bmatrix} \tag{2.21}$$

This equation has four sets of unknowns, the correction factors for voltages at 'Q', the voltages at 'R', and currents from either end of the line. This equation alone would not lead to the correct correction factors. However equation (2.20) helps us to estimate the calibrated voltage at bus 'Q'. This information can be applied to equation (2.21) to help estimate the remaining correction factors. This results in the requirement of a network of measurements that are connected to the perfectly calibrated instrument transformer.

Subsequently the equations for the rest of the system can be developed similarly. For example, for the next set of buses ‘R’ and ‘S’:

$$\begin{bmatrix} zero(3,1) \\ zero(3,1) \\ . \\ . \\ . \\ zero(3,1) \\ zero(3,1) \end{bmatrix} = \begin{bmatrix} -Y_{rs}^{abc}V_{r1}^{abc} & (Y_{rs}^{abc}+B_{s0}^{abc})diag(V_{s1}^{abc}) & zero(3,3) & -diag(I_{sr1}^{abc}) \\ -(Y_{rs}^{abc}+B_{r0}^{abc})V_{r1}^{abc} & Y_{rs}^{abc}diag(V_{s1}^{abc}) & diag(I_{rs1}^{abc}) & zero(3,3) \\ . & . & . & . \\ . & . & . & . \\ . & . & . & . \\ -Y_{rs}^{abc}V_{rn}^{abc} & (Y_{rs}^{abc}+B_{s0}^{abc})diag(V_{sn}^{abc}) & zero(3,3) & -diag(I_{sr1}^{abc}) \\ -(Y_{rs}^{abc}+B_{r0}^{abc})V_{rn}^{abc} & Y_{rs}^{abc}diag(V_{sn}^{abc}) & diag(I_{rs1}^{abc}) & zero(3,3) \end{bmatrix} \begin{bmatrix} K_{vq}^{abc} \\ K_{vr}^{abc} \\ K_{iqr}^{abc} \\ K_{irq}^{abc} \end{bmatrix} \quad (2.22)$$

Therefore by progressing along the connected tree and applying the least squares estimation process using the previously calibrated values, we can estimate correction factors for all the buses that are connected to the perfect measurement.

2.3.1 Simulations on a System Model Subset

To observe the results of the calibration method on a multi bus system, a small subset of a real system model was considered. Since sufficient real time synchrophasor data was not available, a PSS/E model was used to generate the data. A subset of the system consisting of 6 buses and 5 lines was used for this study. One of the buses within this system is assumed to have a well calibrated transformer, but subsequent buses connected to this bus are assumed to not have reliable synchrophasor data available.

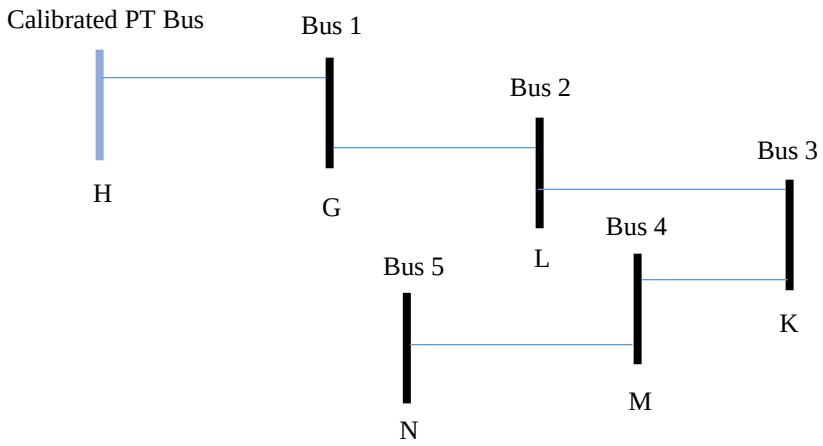

Figure 2.3: A Six Bus Subset of a Real Network

The picture above depicts the connection between the six buses. Similar to the two bus example, errors were applied to the original voltages and currents for the network in figure 2.3. The calibration process was then applied. A larger number of sample load cases were considered for this problem to ensure that the system is not under-defined. Since we know the errors being applied to the original values, we can easily compute the errors in the estimated correction factors. Figures 2.4 and 2.5 show the errors in estimated correction factors of the voltage transformers for different buses:

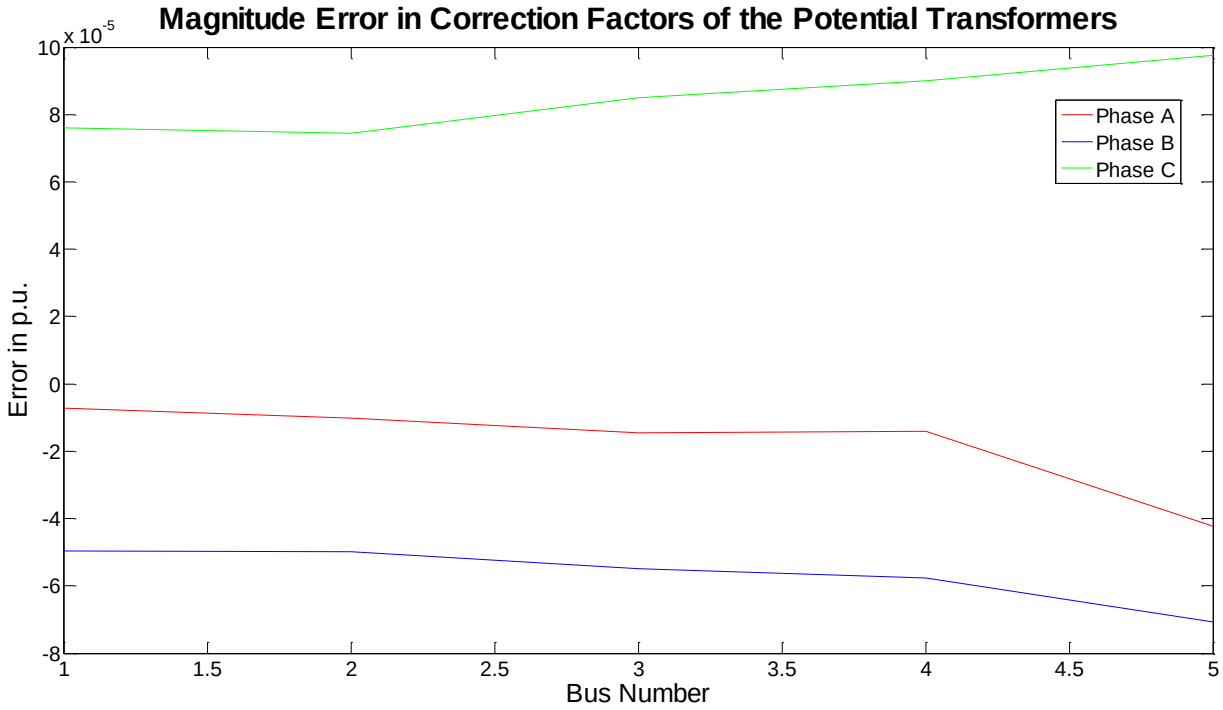

Figure 2.4: Errors in Correction Factors (Magnitude) of PTs Vs Bus Number (away from perfect measurement)

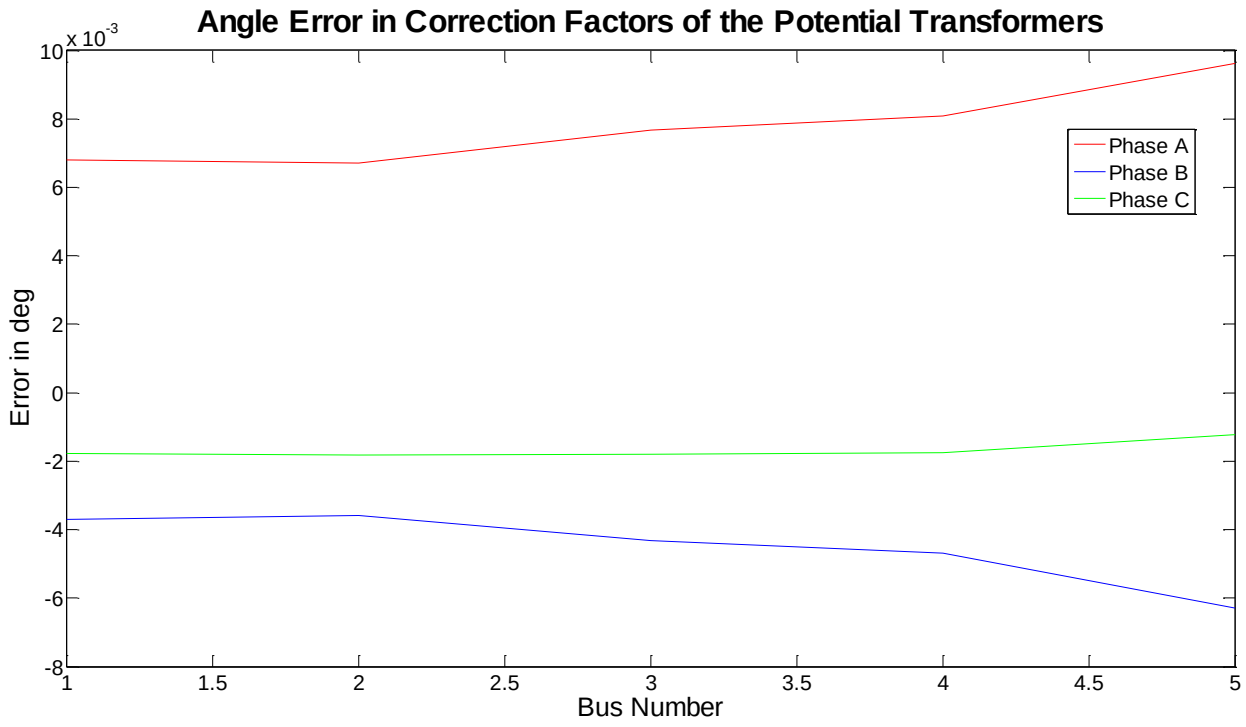

Figure 2.5: Errors in Correction Factors (Angle) of PTs Vs Bus Number (away from perfect measurement)

For the voltage measurements, it is interesting to note how the error seems to increase as we move further away from the perfectly calibrated transformer. For this particular system the error remains within an acceptable range (<1%) but this point should be kept in mind when performing calibration on a much larger system. With the presence of multiple well calibrated measurements on the network, this problem could be mitigated.

When observing the errors of the correction factors of the current transformers, they appear to remain within a fixed range as we move across the lines, although being larger than the errors of the potential transformers' correction factors. In the following figures the branch numbers 1 through 5 indicate current measured in the positive direction (Ipq) of the line and branches 6 to 10 indicate the currents measured from the opposite end (Iqp).

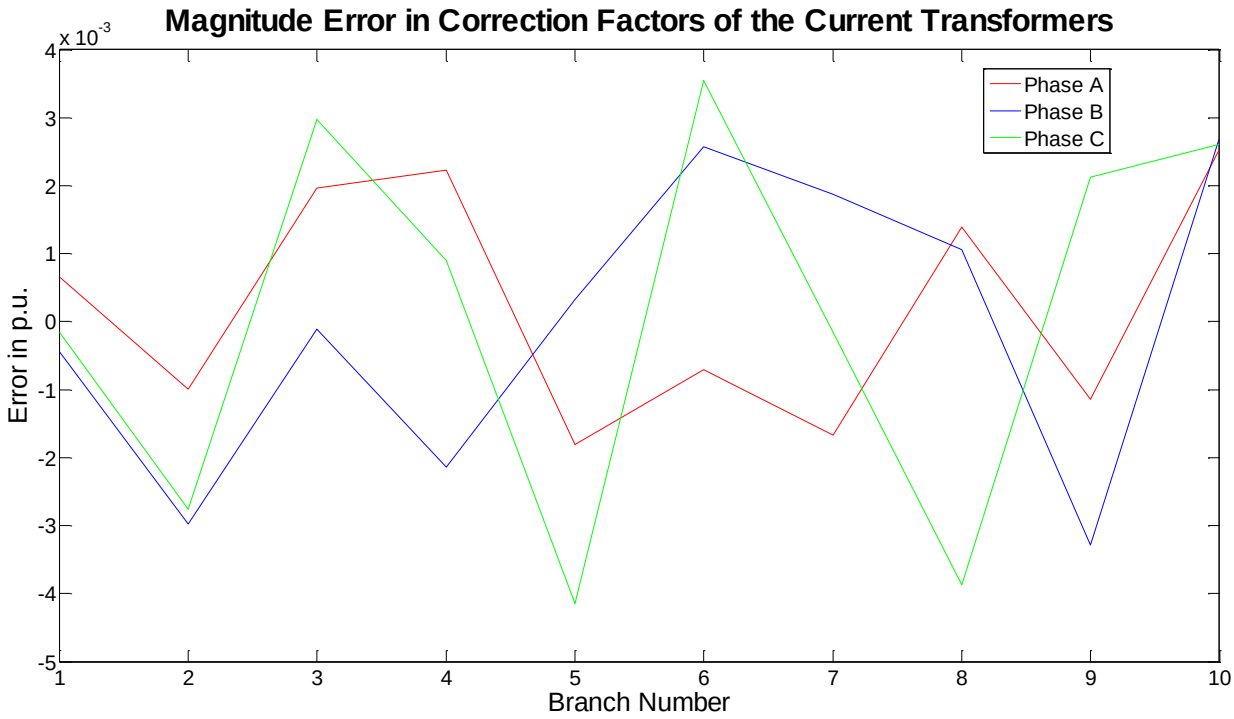

Figure 2.6: Errors in Correction Factors (Magnitude) of CTs Vs Branch Number

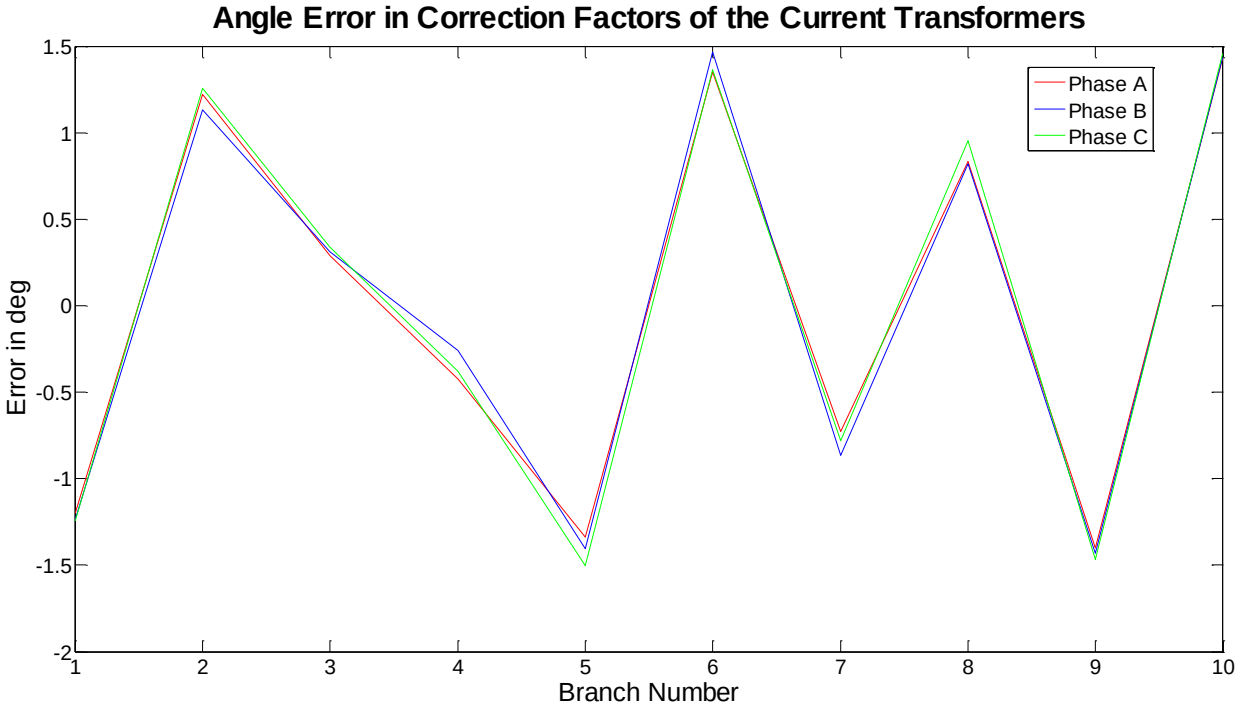

Figure 2.7: Errors in Correction Factors (Angle) of CTs Vs Branch Number

Chapter 3: Line Parameter Estimation using the Kalman Filter

3.1 The Kalman Filter

Named after Dr. Rudolf E. Kalman, this filtering algorithm was initially developed in 1960. Also known as linear quadratic estimation, the method uses a series of measurements observed over time to predict the next state of the system. The method has been proven to work well in the presence of statistical errors and noise, oftentimes better than methods that only use a single measurement.

With the filter finding applications across a spectrum of applications such as trajectory optimization, guidance, navigation, control, signal processing, econometrics, state estimation, different variants of the method have evolved, in order to aid computations for specific types of problems. Some of these include the Kalman-Bucy Filter, the Extended Kalman filter, the Hybrid Kalman filter, the Information Kalman filter, to name a few.

The core algorithm essentially works in two steps: predict and correct. In the predict step, the algorithm estimates the state of the system and its uncertainties based on the current measurement. In the correct step, the algorithm uses the next measurement, compares it to the previous value estimated by the algorithm, and makes necessary corrections to the estimation process to improve the next estimate. The successive estimate produced by the filter is then a weighted average of the new measurement and the system prediction. Weights are allotted during the update process, with better estimates obtaining greater weights. This process is repeated for each new supply measurement. The method is thus recursive, requiring only the new measurement at each iteration and no storage of previous measurements.

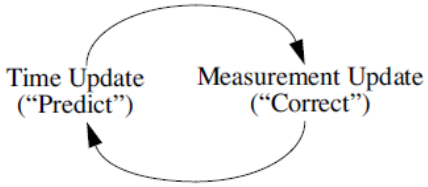

Figure 3.1 : The predict and correct algorithm [26]

3.2 A Closer Look

Let x_k be the state of the system at instant k, and x_{k-1} be its state at instant $k-1$. The state of the system evolves according to the expression:

$$x_k = F_k x_{k-1} + B_k u_k + w_k \tag{3.1}$$

Where F_k : the state transition matrix

B_{k-1} : the set of control inputs

u_k : the input vector model

w_k : the process noise

The process noise w_k is assumed to be drawn from a multivariate Gaussian distribution with mean zero and covariance Q_k, i.e. $w_k \sim \boldsymbol{N}(0, Q_k)$.

An observation z_k of the state x_k can then be described according to:

$$z_k = H_k x_k + v_k \tag{3.2}$$

Where H_k : maps the true state space model onto the observation space

v_k : the observation noise

The observation noise is also assumed to be zero mean and Gaussian with covariance R_k, i.e. $v_k \sim N(0, R_k)$.

Two variables are important when building the filter: $\hat{x}_{k|k}$ an estimate of the (current) state given all observations up to and including instant k, and $P_{k|k}$, the error covariance matrix. $P_{k|k}$ gives us an idea of the estimated accuracy of the filter.

As described previously, the Kalman filter algorithm can be conceptualized through two stages, 'predict' and 'correct'. The 'predict' stage uses the prior state estimate to compute a state estimate at the current time instant. This estimate is also known as the *a priori estimate*. It does not take into account any current observation. The resulting state estimate and error covariance can be given by:

$$\hat{x}_{k|k-1} = F_k \hat{x}_{k-1|k-1} + B_{k-1} u_{k-1} \tag{3.3}$$

$$P_{k|k-1} = F_k P_{k-1|k-1} F_k^T + Q_k \tag{3.4}$$

During the 'correct' stage, the observation from the current time step is considered and used to refine the final state estimate. This results in the *a posteriori estimate*. The new observation is used to compute the measurement residual $\tilde{y}_k$ and the residual covariance S_k which can then be used to get the optimal Kalman gain, given by K_k.

$$\tilde{y}_k = z_k - H_k \hat{x}_{k|k-1} \tag{3.5}$$

$$S_k = H_k P_{k|k-1} H_k^T + R_k \tag{3.6}$$

$$K_k = P_{k|k-1}\, H_k^T S_k^{-1} \tag{3.7}$$

Once the Kalman gain is computed the *a posteriori* estimate and the *a posteriori* covariance are:

$$\hat{x}_{k|k} = \hat{x}_{k|k-1} + K_k \tilde{y}_k \tag{3.8}$$

$$P_{k|k} = (I - K_k H_k) P_{k|k-1} \tag{3.9}$$

Usually the algorithm progresses with the 'predict' and 'correct' stages alternating. In the event a new observation is not available, the 'correct' step may be skipped, and multiple

predictions may be made. In case there are several observations available for a single instant, multiple corrections can also be used, assuming appropriately different observation models (H_k). A more detailed picture of figure 3.1 can be seen in the following diagram.

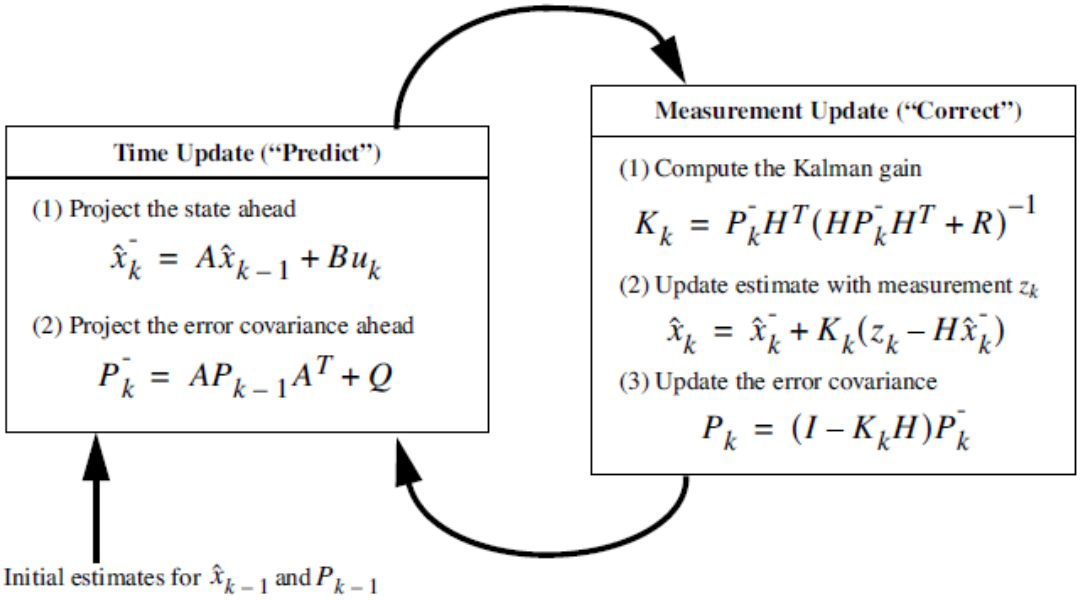

Figure 3.2 : A detailed picture of the Kalman Filter [26]

3.3 Using the Kalman filter to estimate line parameters

A method to estimate three phase line parameters with Kalman filtering has been developed in the reference [27]. The method employed is explained in the following sections.

Consider a two bus system connected via a three phase line as described earlier.

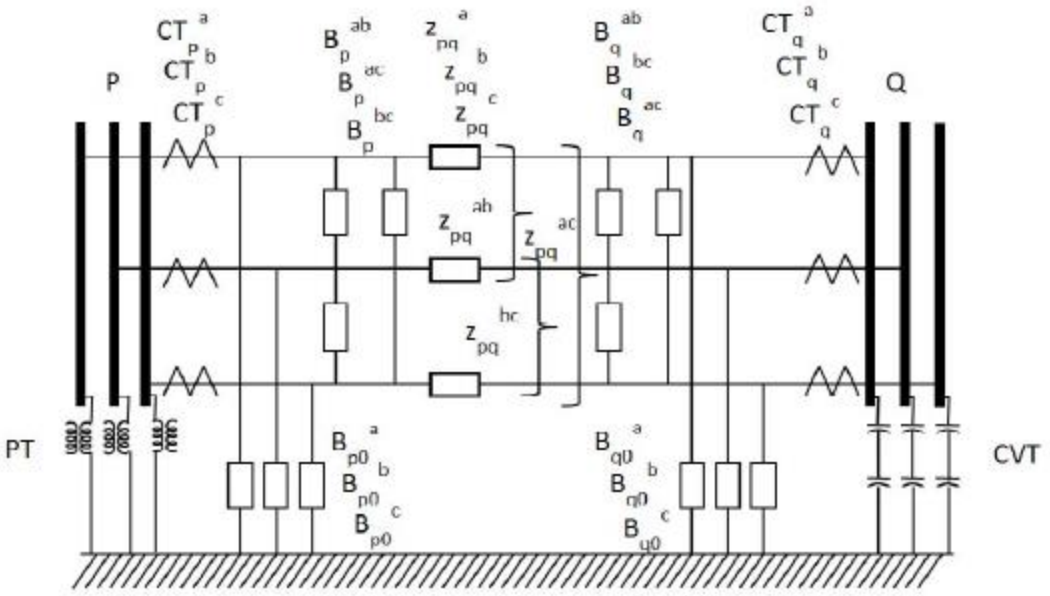

Figure 3.3 : A two bus three phase system

The line has its three phase impedance described by,

$$Z_{pq}^{abc} = \begin{bmatrix} Z_{pq}^{a} & Z_{pq}^{ab} & Z_{pq}^{ac} \\ Z_{pq}^{ab} & Z_{pq}^{b} & Z_{pq}^{bc} \\ Z_{pq}^{ac} & Z_{pq}^{bc} & Z_{pq}^{c} \end{bmatrix} \tag{3.10}$$

and line admittance by,

$$Y_{pq}^{abc} = (Z_{pq}^{abc})^{-1} = \begin{bmatrix} Y_{pq}^{a} & Y_{pq}^{ab} & Y_{pq}^{ac} \\ Y_{pq}^{ab} & Y_{pq}^{b} & Y_{pq}^{bc} \\ Y_{pq}^{ac} & Y_{pq}^{bc} & Y_{pq}^{c} \end{bmatrix} \tag{3.11}$$

The susceptances at either ends of the line can be described by

$$B_{p0}^{abc} = j \begin{bmatrix} B_{p0}^{a} + B_{p0}^{ab} + B_{p0}^{ac} & -B_{p0}^{ab} & -B_{p0}^{ac} \\ -B_{p0}^{ab} & B_{p0}^{b} + B_{p0}^{ba} + B_{p0}^{bc} & -B_{p0}^{bc} \\ -B_{p0}^{ac} & -B_{p0}^{bc} & B_{p0}^{c} + B_{p0}^{ca} + B_{p0}^{cb} \end{bmatrix} \tag{3.12}$$

$$B_{q0}^{abc} = j\begin{bmatrix} B_q^a + B_{q0}^{ab} + B_q^{ac} & -B_{q0}^{ab} & -B_{q0}^{ac} \\ -B_{q0}^{ab} & B_{q0}^{b} + B_{q0}^{ba} + B_{q0}^{bc} & -B_{q0}^{bc} \\ -B_{q0}^{ac} & -B_{q0}^{bc} & B_{q0}^{c} + B_{q0}^{ca} + B_{q0}^{cb} \end{bmatrix} \tag{3.13}$$

The p, q subscripts refer to bus index, a, b, c subscripts refer to phase index, and 0 refers to ground.

We know that the voltages at either end of the line can be expressed by:

$$V_q^{abc} = V_p^{abc} - Z_{pq}^{abc}(I_{pq}^{abc} - B_{p0}^{abc} * V_p^{abc}) \tag{3.14}$$

$$V_p^{abc} = V_q^{abc} - Z_{pq}^{abc}(I_{qp}^{abc} - B_{q0}^{abc} * V_q^{abc}) \tag{3.15}$$

where V_p^{abc} : three phase voltage at 'P'

V_q^{abc} : three phase voltage at 'Q'

I_{pq}^{abc} : three phase currents flowing from 'P' to 'Q'

I_{qp}^{abc} : three phase currents flowing from 'Q' to 'P'

Rearranging the terms of (3.14) and (3.15), we have

$$Y_{pq}^{abc}\left(V_p^{abc} - V_q^{abc}\right) = I_{pq}^{abc} - B_{p0}^{abc}V_p^{abc} \tag{3.16}$$

$$Y_{pq}^{abc}\left(V_q^{abc} - V_p^{abc}\right) = I_{qp}^{abc} - B_{q0}^{abc}V_q^{abc} \tag{3.17}$$

Summing (3.16) and (3.17), we get an expression that is independent of Y_{pq}^{abc}.

$$I_{pq}^{abc} + I_{qp}^{abc} = B_{p0}V_p + B_{q0}V_q \tag{3.18}$$

In three phase notation,

$$\begin{bmatrix} I_{pq}^{a} + I_{qp}^{a} \\ I_{pq}^{b} + I_{qp}^{b} \\ I_{pq}^{c} + I_{qp}^{c} \end{bmatrix} = \begin{bmatrix} V_p^a & 0 & 0 & V_p^a - V_p^b & 0 & V_p^a - V_p^c & V_q^a & 0 & 0 & V_q^a - V_q^b & 0 & V_q^a - V_q^c \\ 0 & V_p^b & 0 & V_p^b - V_p^a & V_p^b - V_p^c & 0 & 0 & V_q^b & 0 & V_q^b - V_q^a & V_q^b - V_q^c & 0 \\ 0 & 0 & V_p^c & 0 & V_p^c - V_p^b & V_p^c - V_p^a & 0 & 0 & V_q^c & 0 & V_q^c - V_q^b & V_q^c - V_q^a \end{bmatrix} * j \begin{bmatrix} B_{p0}^{a} \\ B_{p0}^{b} \\ B_{p0}^{c} \\ B_{p0}^{ab} \\ B_{p0}^{bc} \\ B_{p0}^{ca} \\ B_{q0}^{a} \\ B_{q0}^{b} \\ B_{q0}^{c} \\ B_{q0}^{ab} \\ B_{q0}^{bc} \\ B_{q0}^{ca} \end{bmatrix} \tag{3.19}$$

Seeing that equation (3.19) is independent of impedances, we can use it to estimate the susceptances through a Kalman filter implementation. Rewriting (3.19),

$$I_{sus} = V_{sus} * B_{sus} \tag{3.20}$$

Where I_{sus} is the LHS of equation (3.19) and V_{sus} is the matrix multiplied by the column of susceptances, B_{sus} on the RHS. Now since these are complex quantities, we separate the real and imaginary portions to get:

$$\begin{bmatrix} Re(I_{sus}) \\ Im(I_{sus}) \end{bmatrix} = \begin{bmatrix} -Im(V_{sus}) \\ Re(V_{sus}) \end{bmatrix} [B_{sus}] \tag{3.21}$$

Note that B_{sus} consists of purely imaginary quantities. In keeping with the notation developed earlier, equation (3.21) can be written as:

$$z_{sus} = H_{sus}\, x_{sus} + v_{sus} \tag{3.22}$$

Now the Kalman filter model to estimate the susceptances would be as follows:

$$\hat{x}_{k|k-1} = \hat{x}_{k-1|k-1} \tag{3.23}$$

$$P_{k|k-1} = P_{k-1|k-1} \tag{3.24}$$

$$K_k = P_{k|k-1} * H_k^T * \left(H_k * P_{k|k-1} * H_k^T + R\right)^{-1} \quad (3.25)$$

$$\hat{x}_{k|k} = \hat{x}_{k|k-1} + K_k * (z_k - H_k * \hat{x}_{k|k-1}) \quad (3.26)$$

$$P_{k|k} = (I - K_k * H_k) P_{k|k-1} \quad (3.27)$$

R in (3.25) is the error covariance matrix. A more detailed development of this can be found in the appendix A. I is the identity matrix. With an adequate number of samples. We can use the model developed above to estimate the line susceptance matrix, B_{sus} . This in turn can be used to estimate the impedances in the following way. From equation (3.14), we have:

$$V_p^{abc} - V_q^{abc} = Z_{pq}^{abc}(I_{pq}^{abc} - B_{p0}^{abc} * V_p^{abc}) \quad (3.28)$$

In three phase,

$$\begin{bmatrix} V_p^a - V_q^a \\ V_p^b - V_q^b \\ V_p^c - V_q^c \end{bmatrix} = \begin{bmatrix} m_1 & 0 & 0 & m_2 & 0 & m_3 \\ 0 & m_2 & 0 & m_1 & m_3 & 0 \\ 0 & 0 & m_3 & 0 & m_2 & m_1 \end{bmatrix} \begin{bmatrix} Z_{pq}^a \\ Z_{pq}^b \\ Z_{pq}^c \\ Z_{pq}^{ab} \\ Z_{pq}^{bc} \\ Z_{pq}^{ca} \end{bmatrix} \quad (3.29)$$

Where $m_1 = I_{pq}^a - j[B_{p0}^a + B_{p0}^{ab} + B_{p0}^{ac} \quad - B_{p0}^{ab} \quad - B_{p0}^{ca}]$

$m_2 = I_{pq}^b - j[B_{p0}^{ba} \quad B_{p0}^b + B_{p0}^{ba} + B_{p0}^{bc} \quad - B_{p0}^{bc}]$

$m_3 = I_{pq}^c - j[-B_{p0}^{ac} \quad - B_{p0}^{bc} \quad B_{p0}^c + B_{p0}^{ca} + B_{p0}^{cb}]$

We can write (3.29) in the following way:

$$V_{imp} = I_{imp} * Z_{imp} \quad (3.30)$$

Where V_{imp} forms the LHS and I_{imp} is the matrix that is multiplied by the impedance vector, Z_{imp}. Separating the real and imaginary terms, we get:

$$\begin{bmatrix} Re(V_{imp}) \\ Im(V_{imp}) \end{bmatrix} = \begin{bmatrix} Re(I_{imp}) & -Im(I_{imp}) \\ Im(I_{imp}) & Re(I_{imp}) \end{bmatrix} \begin{bmatrix} Re(Z_{imp}) \\ Im(Z_{imp}) \end{bmatrix} \tag{3.31}$$

(3.31) can be expressed by:

$$z_{imp} = H_{imp} * x_{imp} \tag{3.32}$$

Now using the Kalman filter equations developed in (3.23) through (3.27), and plugging in the values of estimated susceptances from the previous stage, we can estimate the impedance vector.

3.4 Observing the Method's Results

3.4.1 A Two Bus System with Significant Loading Variation

To better understand how the Kalman filter could be used for our study, let us consider a system of two buses connected via a transmission line. The first case studied is a randomly varying dataset. This can be assumed to be similar to sample points taken at different points in a day at two buses where the load fluctuates considerably. The voltages and currents considered are as follows.

Vp					
Phase A		Phase B		Phase C	
Mag. (p.u.)	Angle (deg)	Mag. (p.u.)	Angle (deg)	Mag. (p.u.)	Angle (deg)
1	0	1	30	1	-90
1.05	-90	1.05	120	1.05	-30
0.95	45	0.95	120	0.95	90
0.97	45	0.97	-22.5	0.97	90
1.01	30	1.01	36	1.01	60
1.03	0	1.03	18	1.03	120
1.1	90	1.1	-180	1.1	-90
1.02	22.5	1.02	-45	1.02	180
0.99	-45	0.99	90	0.99	-90
0.96	-90	0.96	120	0.96	60
0.97	30	0.97	-90	0.97	0
0.98	120	0.98	-30	0.98	-90
1.03	120	1.03	90	1.03	45
1.02	-22.5	1.02	90	1.02	45
0.99	36	0.99	60	0.99	30
0.975	18	0.975	120	0.975	0
1.015	-180	1.015	-90	1.015	90
0.995	-45	0.995	180	0.995	22.5
1	90	1	-90	1	-45
1.02	120	1.02	60	1.02	-90

Table 3.1: Voltages at bus ‘P’

Vq					
Phase A		Phase B		Phase C	
Mag. (p.u.)	Angle (deg)	Mag. (p.u.)	Angle (deg)	Mag. (p.u.)	Angle (deg)
0.95	0	0.95	30	0.95	-180
1	-90	1	120	1	60
0.9	45	0.9	120	0.9	-90
1.01	22.5	1.01	90	1.01	45
1.02	-45	1.02	-15	1.02	-90
1.05	120	1.05	-120	1.05	0
0.97	60	0.97	-22.5	0.97	30
0.9	18	0.9	-30	0.9	25.7143
0.92	180	0.92	120	0.92	180
0.99	0	0.99	-180	0.99	120
0.97	-180	0.97	30	0.97	0
1.02	60	1.02	120	1.02	-90
1.01	-90	1.01	120	1.01	45
0.98	45	0.98	90	0.98	22.5
0.96	-90	0.96	-15	0.96	-45
1	0	1	-120	1	120
0.98	30	0.98	-22.5	0.98	60

0.99	25.7143	0.99	-30	0.99	18
1	180	1	120	1	180
0.9	120	0.9	-180	0.9	0

Table 3.2: Voltages at bus 'Q'

Using the above dataset, we apply the Kalman filter methodology described previously in order to estimate the line parameters. With successive iterations, the algorithm's estimation is shown to improve. Plotted below are the tolerances, i.e. the differences between consecutive estimates for the susceptances and the impedances.

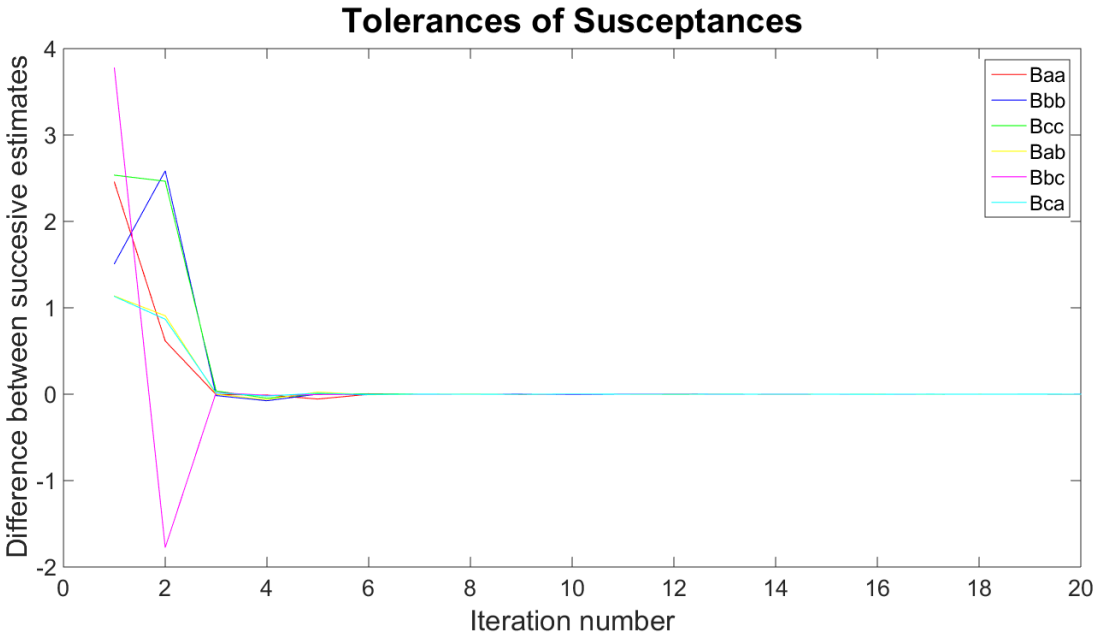

Figure 3.4 : Convergence of susceptance estimation

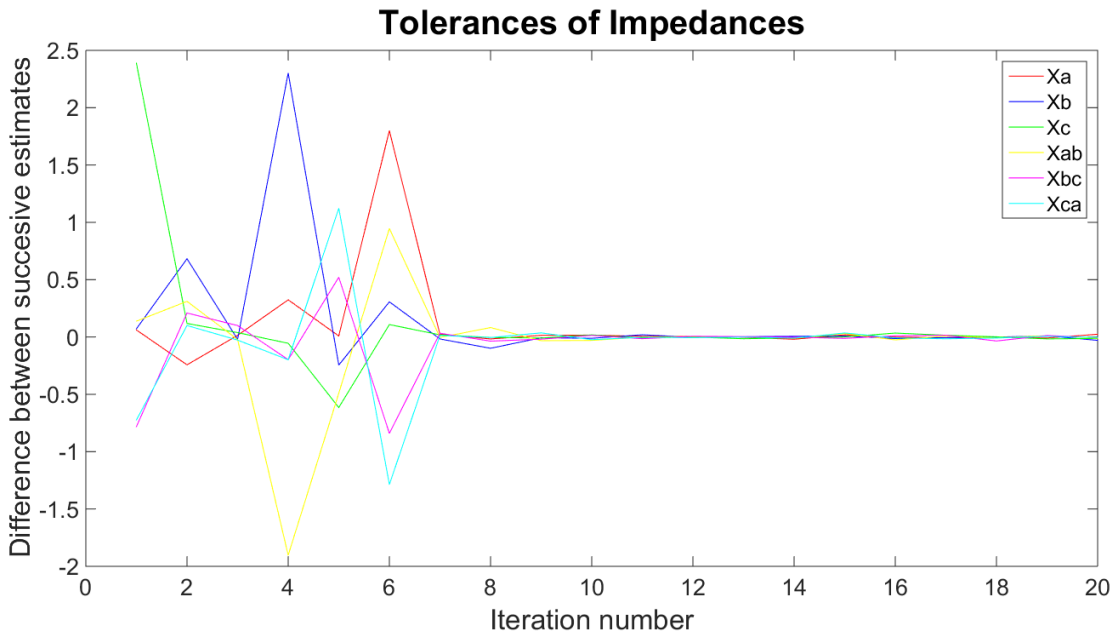

Figure 3.5 : Convergence of impedance estimation

As we can see, both the estimation processes converge within ten iterations. As expected, this can vary depending on the errors present on the measurements, and the estimation covariance supplied to the Kalman estimator. With no errors applied, i.e. assuming perfect measurements, the error covariance can be assumed to be very small, and the method was found to converge fairly quickly, within 3-4 iterations.

The final estimated values were found to be within an acceptable range of the original parameters. The original value of susceptance was:

$$B_{orig} = \begin{bmatrix} 7i & -2i & -2i \\ -2i & 8i & -2i \\ -2i & -2i & 9i \end{bmatrix}$$

And the estimated value was:

$$B_{est} = \begin{bmatrix} 6.9995i & -2.0003i & -2.0005i \\ -2.0003i & 8.0003i & -1.9999i \\ -2.0005i & -1.9999i & 8.9999i \end{bmatrix}$$

The original value of impedance is:

$$Z_{orig} = \begin{bmatrix} 3+4i & 2i & 2i \\ 2i & 4+5i & 2i \\ 2i & 2i & 3+2i \end{bmatrix}$$

And the estimated value was:

$$Z_{est} = \begin{bmatrix} 3.0181 + 4.0080i & -0.0009 + 1.9923i & -0.0023 + 1.9958i \\ -0.0009 + 1.9923i & 3.9637 + 5.0185i & -0.0127 + 2.0143i \\ -0.0023 + 1.9958i & -0.0023 + 1.9958i & 2.9980 + 2.0086i \end{bmatrix}$$

The Kalman Filter Estimator works quite well in determining the line parameters, as demonstrated above. A point to be noted is that consecutive measurements display sufficient variation, indicating sampling at largely varying load points on the network. In the next section, we shall consider a different dataset, displaying a gradual change in loading.

3.4.2 A Two Bus System with Gradual Load Changes

In the previous section, the voltages and currents were assumed to be sampled at different points of time during a single day, therefore they showed considerable variation. While attempting to determine the susceptances and impedances of a line, temperature is a factor that should be considered, as these parameters are known to vary with temperature. Therefore it seems logical to use samples from a period of time when the temperature is relatively constant for a particular line. Within a day the temperature typically rises and falls with the sun, therefore a window of time needs to be selected for sampling wherein there is a load increase while not much of a temperature increase. The window of 7-8 a.m. could be used for this. However, when sampling within a short and continuous duration of time, it becomes evident that the voltages and their angles do not vary

drastically. This causes some computational difficulties when dealing with the matrices described in the section 3.3. In order to circumvent this, we compute the voltages from the currents, which tend to show sufficient variation. To demonstrate the workaround for this, a dataset small fraction of time with gradual load change has been shown here.

Vp					
Phase A		Phase B		Phase C	
Mag. (p.u.)	Angle (deg)	Mag. (p.u.)	Angle (deg)	Mag. (p.u.)	Angle (deg)
1.0258	-2.22	0.9859	-126.6	0.9936	-246.3
1.0258	-2.7	0.9857	-127.2	0.9929	-246.7
1.0253	-3.73	0.9911	-128.4	0.985	-248.7
1.024	-4.88	0.9838	-129.7	0.9851	-249.2
1.0218	-6.03	0.987	-130.4	0.9897	-250.9
1.018	-7.45	0.9863	-132.1	0.9861	-252.3
1.0203	-6.66	0.9882	-130.9	0.9818	-250.9
1.0224	-5.78	0.9863	-130.2	0.9843	-250.1
1.0241	-4.82	0.988	-128.9	0.9861	-249.4
1.0256	-3.32	0.9865	-127.9	0.9899	-248.2

Table 3.3: Voltages at bus ‘P’

Vq					
Phase A		Phase B		Phase C	
Mag. (p.u.)	Angle (deg)	Mag. (p.u.)	Angle (deg)	Mag. (p.u.)	Angle (deg)
0.9956	-3.99	0.9633	-128.5	0.9616	-248.6
0.9952	-4.89	0.9612	-129	0.9627	-249.8
0.9938	-6.8	0.9621	-131.3	0.9543	-251.3
0.9913	-8.93	0.9556	-133.9	0.9562	-253.3
0.9879	-11.08	0.9576	-135.7	0.9495	-255.4
0.9824	-13.75	0.9516	-138.7	0.9496	-258.1
0.9856	-12.27	0.9478	-136.6	0.9481	-257
0.9887	-10.62	0.9581	-134.8	0.958	-255
0.9915	-8.83	0.9608	-133.3	0.9543	-252.9
0.9944	-6.04	0.9568	-130.6	0.961	-250.8

Table 3.4: Voltages at bus ‘Q’

As described previously, we will use the currents to compute the voltages. The currents at either end of the lines are:

Ipq					
Phase A		Phase B		Phase C	
Mag. (p.u.)	Angle (deg)	Mag. (p.u.)	Angle (deg)	Mag. (p.u.)	Angle (deg)
5.086864	85.89433	7.097846	-36.8708	8.791528	-155.555
5.059954	85.54977	7.098418	-36.7977	8.814415	-156.019
5.064523	84.3784	7.101985	-38.0208	8.811228	-157.2
5.054798	82.98428	7.109965	-39.4335	8.803627	-158.801
5.050188	81.98004	7.118229	-40.7631	8.748371	-160.049
5.042264	80.45411	7.100164	-42.0418	8.75947	-161.388
5.041693	81.09495	7.087112	-41.2141	8.786335	-160.599
5.041906	82.06152	7.084087	-40.5071	8.750138	-159.76
5.040997	83.07957	7.090497	-39.0968	8.810188	-158.61
5.045671	84.68595	7.118994	-37.8549	8.789408	-157.336

Table 3.5: Currents as observed from bus 'P'

Iqp					
Phase A		Phase B		Phase C	
Mag. (p.u.)	Angle (deg)	Mag. (p.u.)	Angle (deg)	Mag. (p.u.)	Angle (deg)
4.914338	84.41946	6.855426	-38.2357	8.529978	-157.126
4.901037	83.528	6.87181	-38.9279	8.556018	-158.208
4.877225	81.66307	6.843578	-40.9304	8.502994	-160.209
4.857802	79.48679	6.873271	-42.9329	8.537851	-162.736
4.852104	77.74302	6.827364	-45.0068	8.456433	-164.283
4.807054	75.0124	6.748454	-47.6108	8.394406	-166.864
4.846784	76.21302	6.76546	-46.5921	8.421582	-165.445
4.859291	77.84549	6.794668	-44.6571	8.484525	-163.762
4.856389	79.66758	6.832426	-42.6553	8.519473	-162.216
4.899804	82.51724	6.884449	-39.9412	8.563063	-159.305

Table 3.6: Currents as observed from bus 'Q'

Now in order to compute the voltages, the EMS values of susceptance and impedance can be used. Equations (3.14) and (3.15) can be rearranged as follows:

$$(1 + Z_{pq}^{abc} B_{p0}^{abc}) V_p^{abc} - V_q^{abc} = Z_{pq}^{abc} I_{pq}^{abc} \quad (3.33)$$

$$(1 + Z_{pq}^{abc} B_{q0}^{abc}) V_q^{abc} - V_p^{abc} = Z_{pq}^{abc} I_{qp}^{abc}) \quad (3.34)$$

In matrix form,

$$\begin{bmatrix} (1 + Z_{pq}^{abc} B_{p0}^{abc}) & -I \\ -I & (1 + Z_{pq}^{abc} B_{p0}^{abc}) \end{bmatrix} \begin{bmatrix} V_p^{abc} \\ V_p^{abc} \end{bmatrix} = \begin{bmatrix} Z_{pq}^{abc} I_{pq}^{abc} \\ Z_{pq}^{abc} I_{qp}^{abc} \end{bmatrix} \quad (3.35)$$

Through equation (3.35) we get a set of voltages. This set of voltages along with the measured currents are then used with the Kalman filter method to estimate the line parameters. Upon performing the workaround described above, the algorithm was found to perform well. The plots showing the convergence of the method can be seen below.

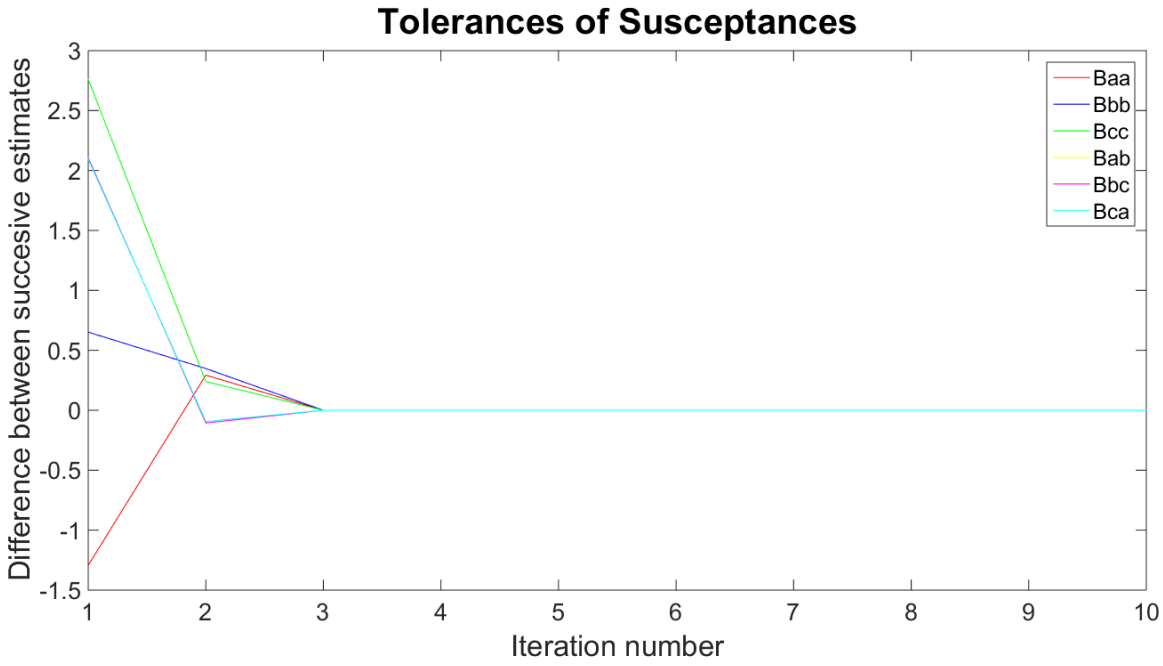

Figure 3.6 : Convergence of susceptance estimation

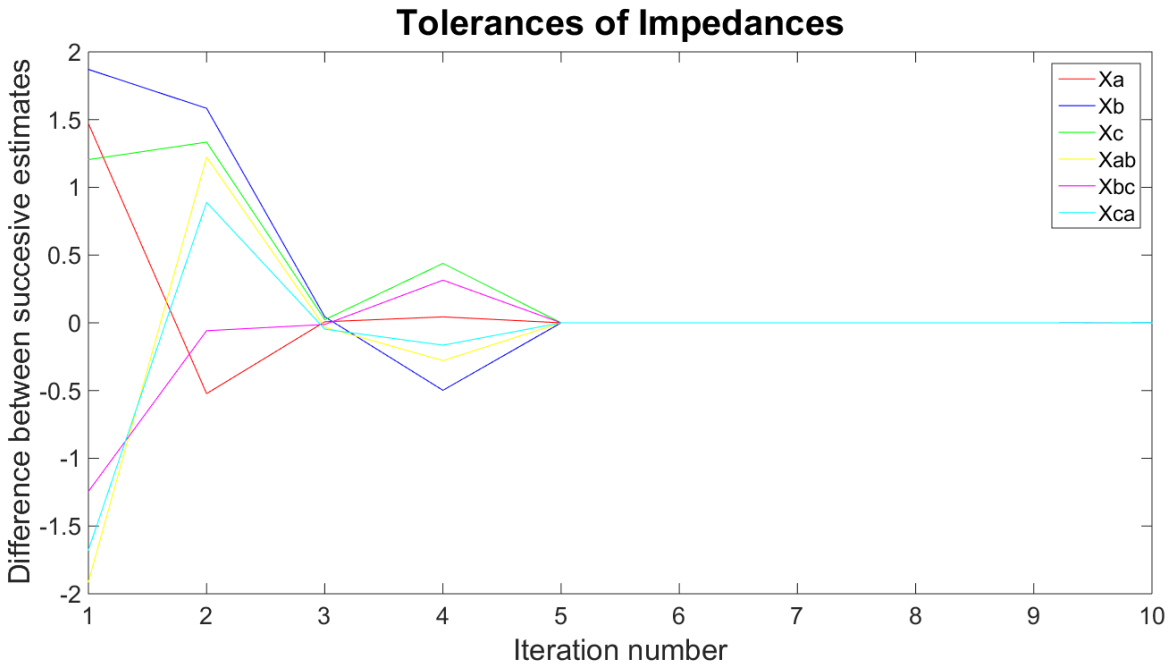

Figure 3.7 : Convergence of impedance estimation

Once again, we can compare the original values of the parameters to the ones estimated by the algorithm. The original value of susceptance was:

$$B_{orig} = \begin{bmatrix} 3i & -2i & -2i \\ -2i & 5i & -2i \\ -2i & -2i & 7i \end{bmatrix}$$

And the estimated value was:

$$B_{est} = \begin{bmatrix} 3i & -2i & -2i \\ -2i & 5i & -2i \\ -2i & -2i & 7i \end{bmatrix}$$

The difference between B_{orig} and B_{est} is in the range of 1e-7. The original value of impedance is:

$$Z_{orig} = \begin{bmatrix} 2+3i & 2i & 2i \\ 2i & 4+3i & 2i \\ 2i & 2i & 4+5i \end{bmatrix}$$

And the estimated value was:

$$Z_{est} = \begin{bmatrix} 1.9999 + 2.9999i & -0.0001 + 2.004i & 0.0003 + 2.0002i \\ -0.0001 + 2.0004i & 4.0010 + 3.0002i & 0.0004 + 1.9992i \\ 0.0003 + 2.0002i & 0.0004 + 1.9992i & 3.9994 + 4.9994i \end{bmatrix}$$

The difference between Z_{orig} and Z_{est} is in the range of 1e-3.
In the following section, the effectiveness of the algorithm on real data collected from the field shall be examined.

3.4.3 Two Bus System with Synchrophasor Data

Since the purpose of our work is to develop a method that can be applied to synchrophasor data, let us consider an actual transmission line. The electric system to which this line belongs has synchrophasors deployed at certain substations across its 500kV network. These synchrophasors transmitted data to a Phasor Data Concentrator, which is where the dataset was obtained from. In order to ensure that the parameters we are trying to estimate were not actually varying due to temperature, the window of 7-8 a.m. has been used. When considering a large system, we should remember that the temperature at different locations may not be the same, but so long as they do not change rapidly within our specific window of study, we should be able to apply the methodology described in the previous section.

For this particular study, as mentioned earlier, the time frame of 7-8 a.m. was examined. The transmission line in question had synchrophasors deployed at either end, and this data was compiled. These synchrophasors were set to report at a rate of 30 samples per second. One second's worth of data was selected for every minute, leaving us with 1800

samples. This data did have missing points as well as 'NaN's, which were subsequently removed, as they would further cause errors. The remaining data consisted of a little over 1700 sample points of voltages and currents in three phase. Typically, the time of 7-8 a.m. comes under the morning load pick up period, where the currents drawn begin to increase but the voltages change gradually. Therefore this dataset was then supplied to the algorithm described in section 3.4.2.

Since there were much more samples being evaluated in this case, a check was employed, in order to improve the efficiency. When the tolerance of the estimators for both the susceptance and impedance fell below an acceptable threshold, the process concludes. The final estimates as compared to the original EMS values are as follows. The original value of susceptance in p.u. was:

$$B_{orig} = \begin{bmatrix} 0.5371i & -0.0896i & -0.1024i \\ -0.0896i & 0.5316i & -0.0505i \\ -0.1024i & -0.0505i & 0.5367i \end{bmatrix}$$

And the estimated value of susceptance in p.u. was:

$$B_{est} = \begin{bmatrix} 0.5370i & -0.0896i & -0.1025i \\ -0.0896i & 0.5316i & -0.0506i \\ -0.1025i & -0.0506i & 0.5366i \end{bmatrix}$$

The difference between B_{orig} and B_{est} is in the range of 1e-7. The original value of impedance in p.u. is:

$$Z_{orig} = \begin{bmatrix} 0.0015 + 0.0141i & 0.0012 + 0.0071i & 0.0012 + 0.0073i \\ 0.0012 + 0.0071i & 0.0015 + 0.0141i & 0.0012 + 0.0066i \\ 0.0012 + 0.0073i & 0.0012 + 0.0066i & 0.0015 + 0.0141i \end{bmatrix}$$

And the estimated value in p.u. was:

$$Z_{est} = \begin{bmatrix} 0.0015 + 0.0141i & 0.0012 + 0.0071i & 0.0012 + 0.0073i \\ 0.0012 + 0.0071i & 0.0015 + 0.0141i & 0.0012 + 0.0066i \\ 0.0012 + 0.0073i & 0.0012 + 0.0066i & 0.0015 + 0.0141i \end{bmatrix}$$

The difference between Z_{orig} and Z_{est} is in the range of 1e-5.

Thus the Kalman Filter was successfully implemented to estimate the transmission line parameters with different sets of data.

Chapter 4: Iterating the Process

When it comes to correctly calibrating instrument transformers and determining the transmission line parameters, it is akin to the chicken-egg problem. In order to correctly calibrate the instrument transformers, the line parameters Z and B are used. If these are erroneous, the calibration results would also be flawed. In the same way, the process of estimating the line parameters described in section 3 assumes that we have a fairly accurate idea of the errors present on the voltage and current measurements, i.e., the measurements have been calibrated. Estimating the parameters without knowing how far the measured values may vary from the true values becomes tricky.

In this scenario, an iterative process could prove beneficial. Let us assume that all the initial values of voltages and currents available are uncalibrated. Similarly the values of impedances and susceptances are also known to have a certain degree of error. Now the instrument transformer calibration process can be performed first, in order to correct the values of the measurements and to estimate the errors present. Following this, the calibrated values can be provided to the line parameter estimation method, resulting in an estimate for Z and B. Now the calibrated values of voltages and currents as well as the estimated impedances and susceptances may still be slightly differing from the true values. But the process can now be repeated, using the estimated Z and B to perform the next round of transformer calibration and successively, the next round of parameter estimation. This process can be repeated as necessary until the tolerance falls below an accepted value, or the estimates stop varying.

It should be mentioned at this point that the process of iterating the two methods until the estimates appear to converge can be implemented with different ways of calibration of transformers and line parameter estimation. During the process of this study, the methods described in the previous chapters were found to work favourably when applied standalone, which is why they were chosen for the overall iterative procedure.

4.1 Testing the method on a Two Bus System

Two buses out of a larger network were considered for this section. A load scaling simulation was performed to obtain different samples. The resulting dataset followed a gradual change in voltage, similar to the dataset in section 3.4.2. The first bus was assumed to have a perfectly calibrated voltage transformer, essential to the calibration process. In this case, the errors were in the order of 10e-2 for magnitudes and 0.05 degrees for the angles. The iterative algorithm was then applied to this dataset. The results obtained are shown below.

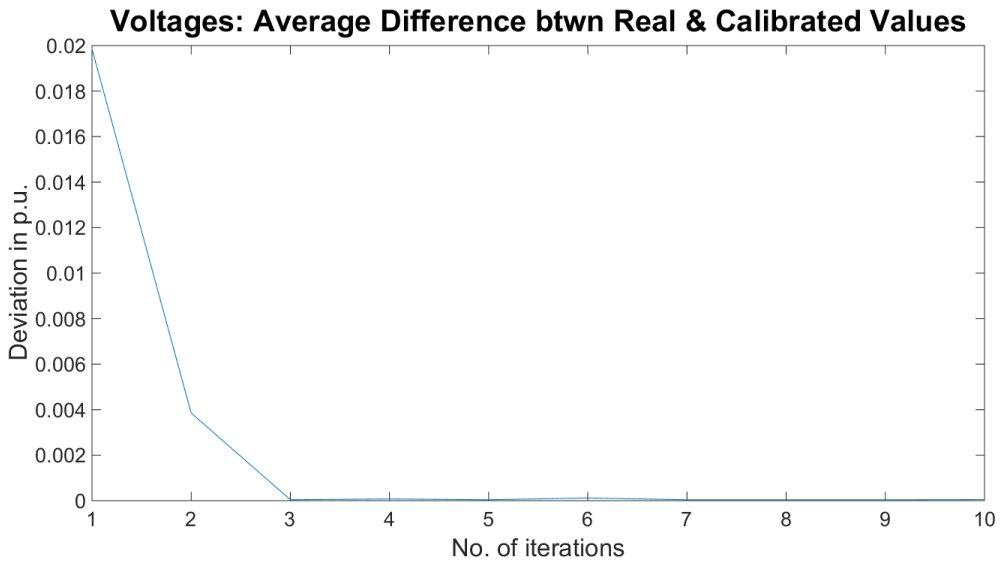

Figure 4.1: Average difference of real and calibrated voltages

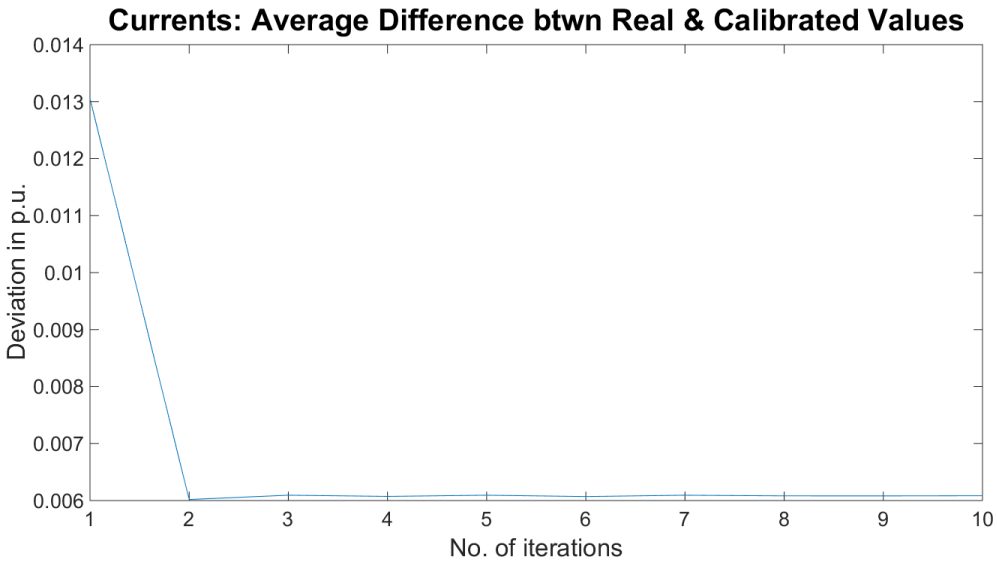

Figure 4.2: Average difference of real and calibrated currents

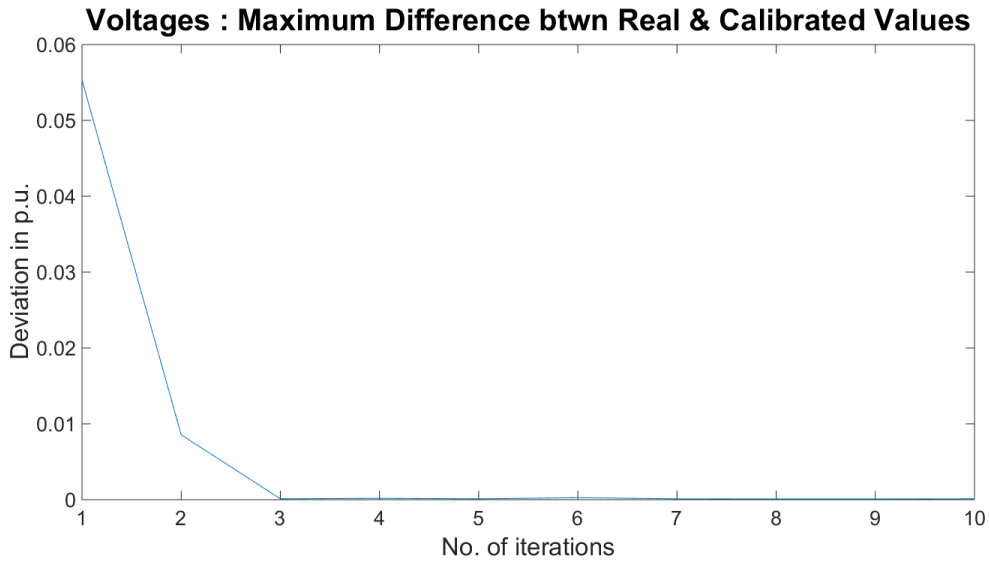

Figure 4.3: Maximum difference of real and calibrated voltages

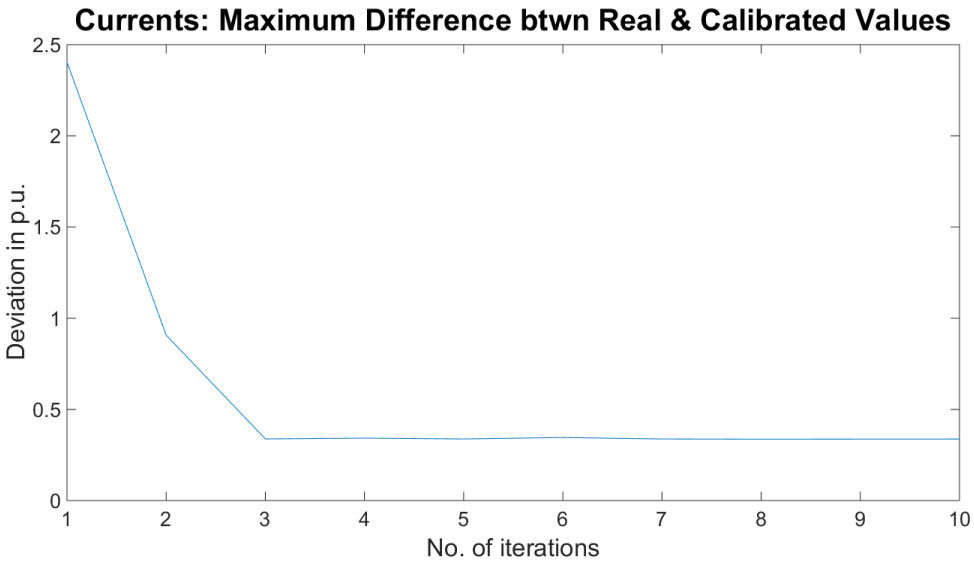

Figure 4.4: Maximum difference of real and calibrated currents

As we can see, the errors in calibration decrease the almost zero. Looking at figure 4.4, we can see that beyond a certain point, the error remains the same when considering the maximum difference between true and calibrated values of currents. Very likely, if there was at least one good current measurement on the system, this would also be close to zero. For the example considered above, only a good voltage measurement was assumed.

The following picture shows how the errors for the individual phases behave.

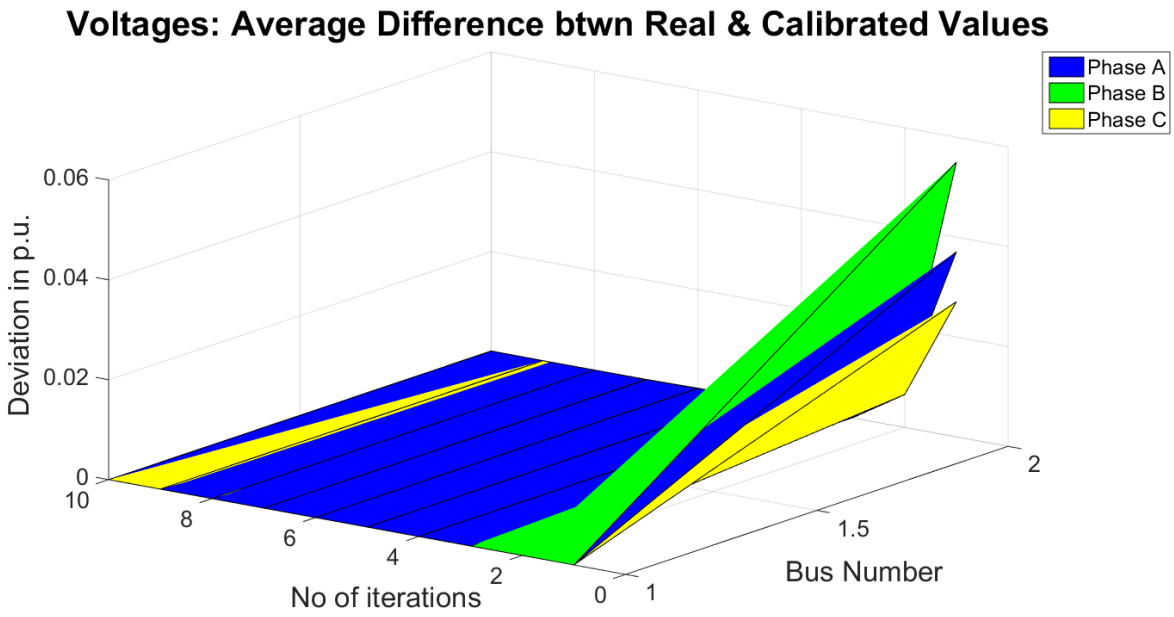

Figure 4.5: Average difference of real and calibrated voltages for each phase

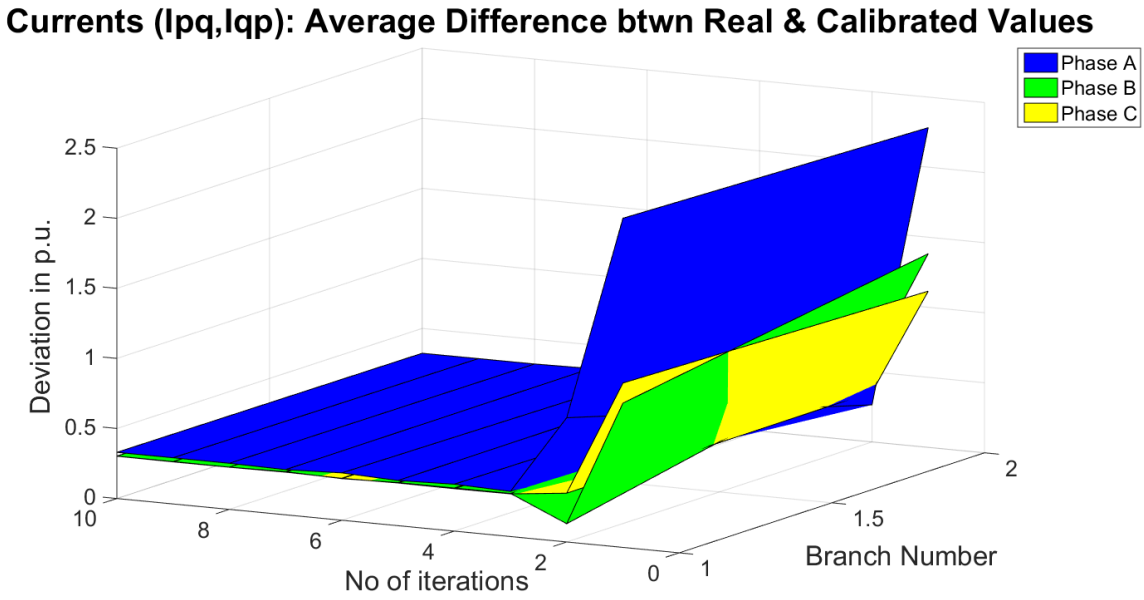

Figure 4.6: Average difference of real and calibrated currents for each phase

As for the line parameters estimation, at the end of 10 iterations, the difference between the true and estimated values of susceptance was in the order of 10e-7, and for impedance it was in the order of 10e-5.

4.2 Testing the method on a Six Bus System

The proposed method was then tested on a six bus system connected through five lines, with the objective of checking whether the calibration and estimation processes still work well with an increased depth of the system. In this case as well, the voltage and current measurements were given an error in the range of 10e-2 for magnitudes and 0.05 degrees for angles. The errors present on the line parameters were in the range of 10%. The results obtained in this case are shown below.

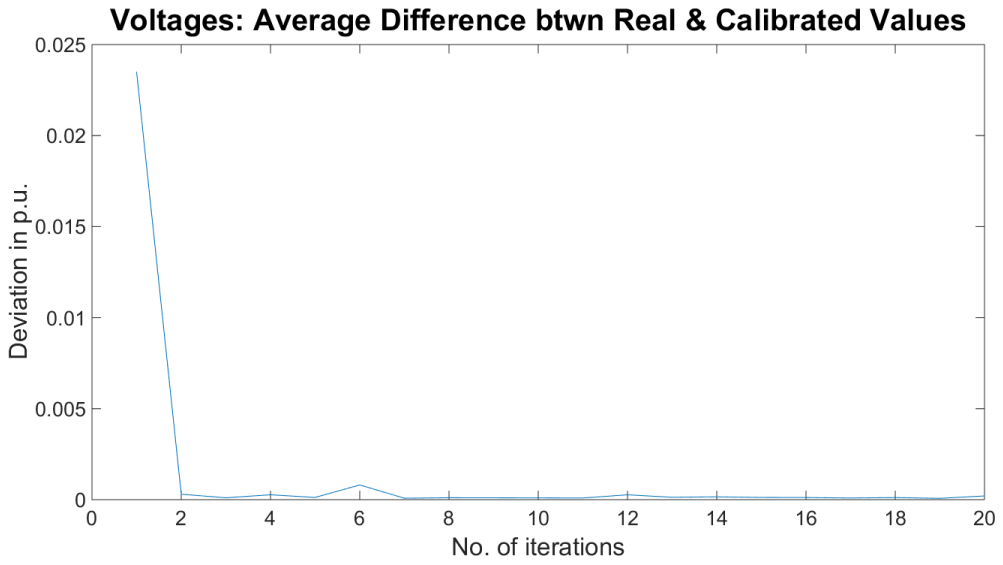

Figure 4.7: Average difference of real and calibrated voltages

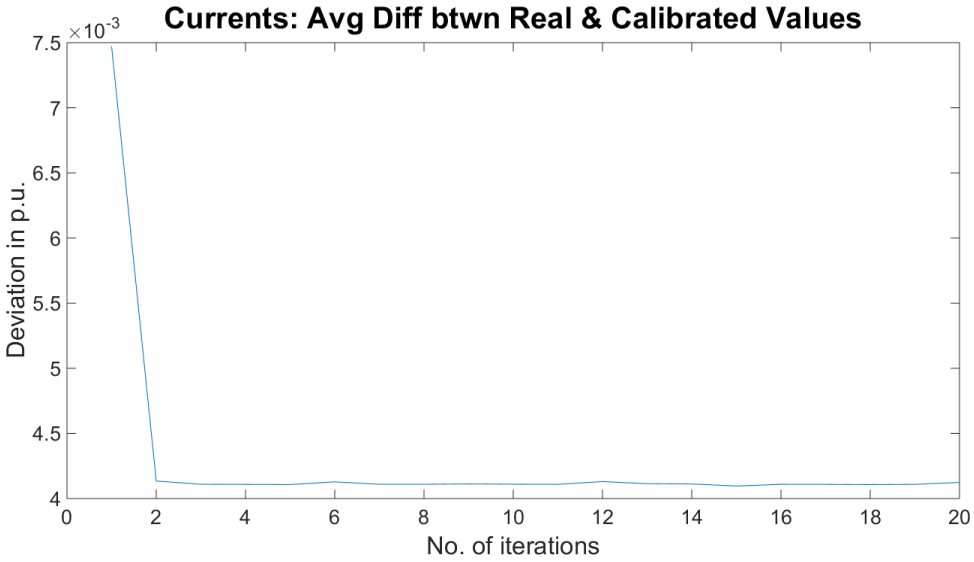

Figure 4.8: Average difference of real and calibrated currents

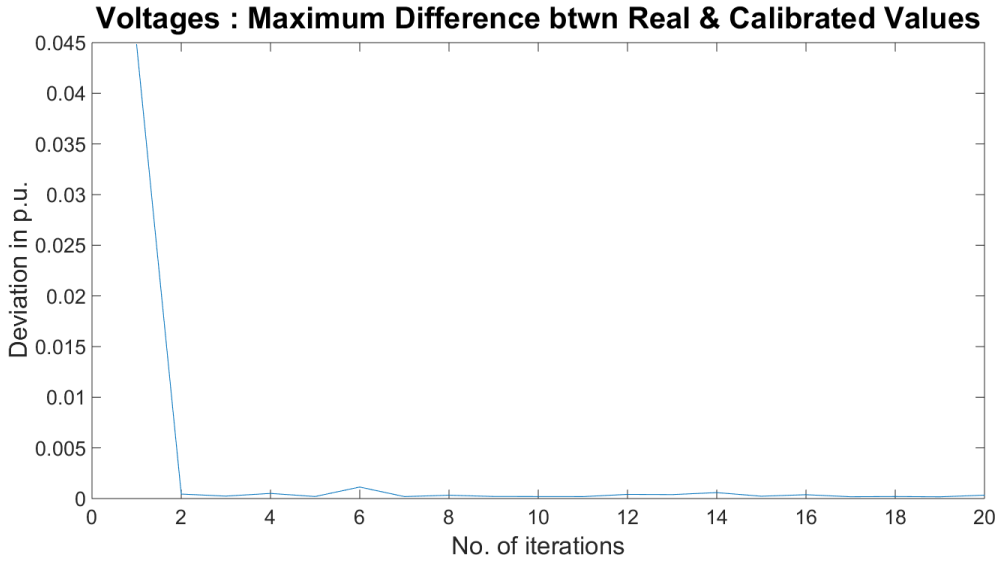

Figure 4.9: Average difference of real and calibrated voltages

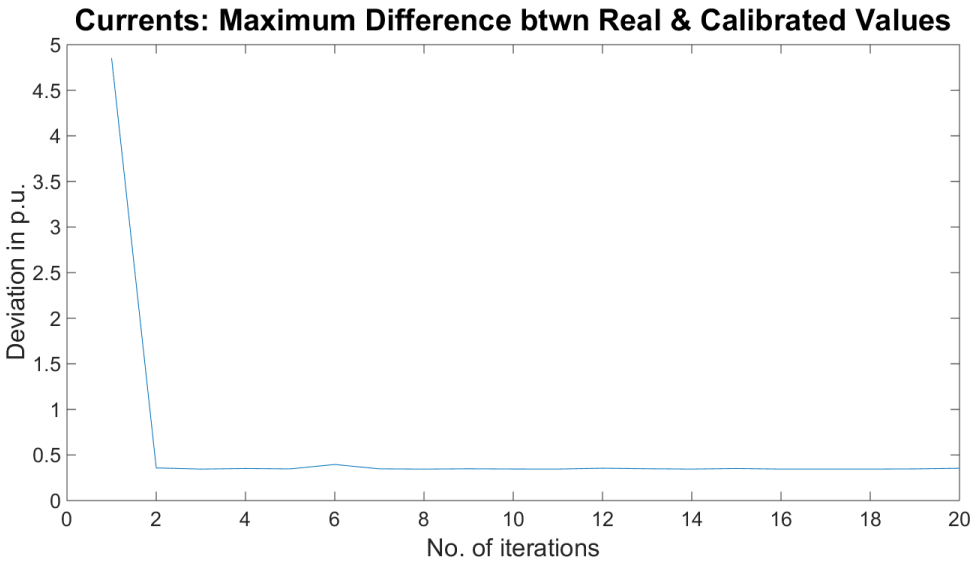

Figure 4.10: Average difference of real and calibrated currents

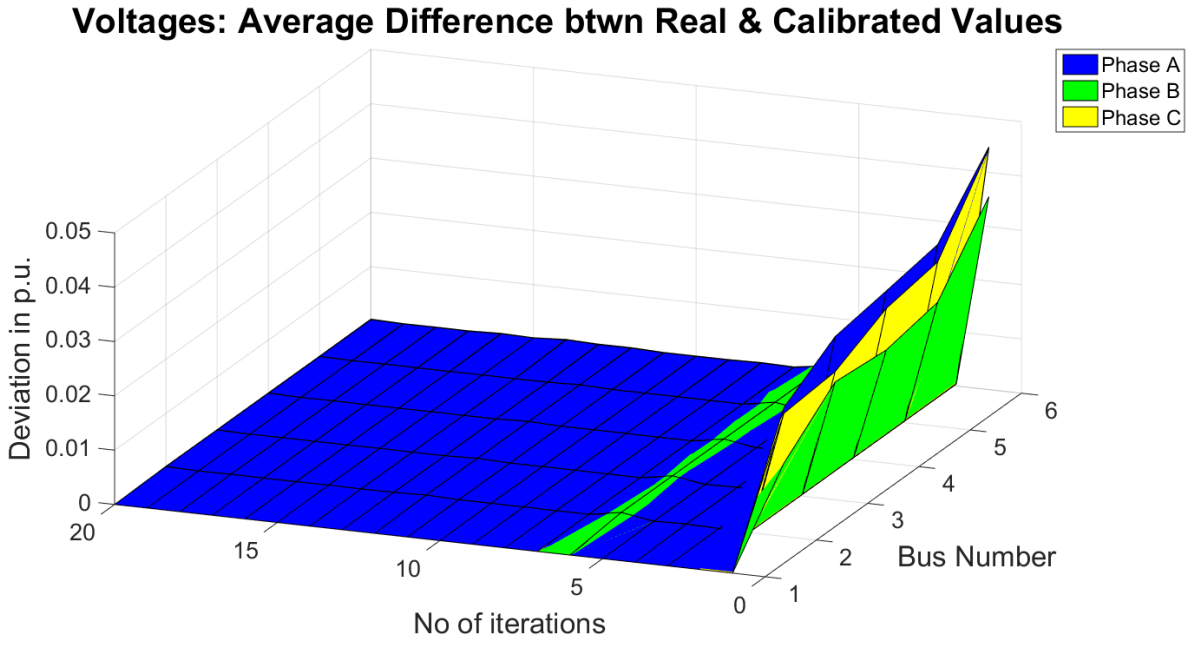

Figure 4.11: Average difference of real and calibrated voltages for each phase

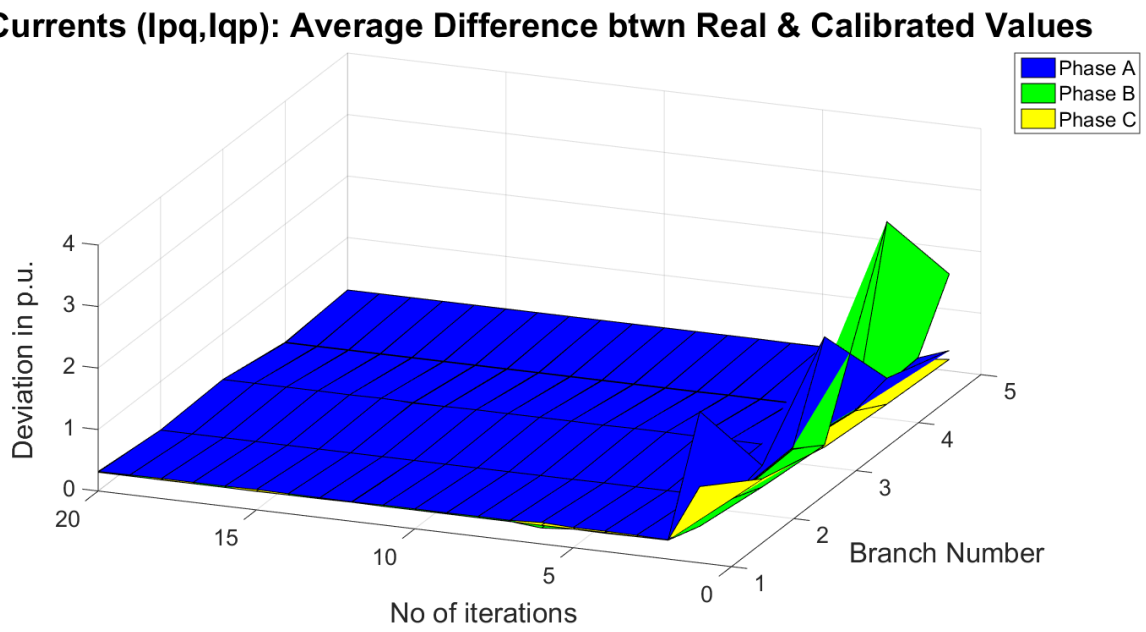

Figure 4.12: Average difference of real and calibrated currents for each phase

Even with a slightly larger system, we can see that the errors converge to near zero in the case of voltages. As for currents, the minimum difference between the true and post-calibration values that can be achieved seems to be about 0.4 p.u. As stated previously, having at least one calibrated current transformer on the network would greatly improve this estimation process. Ideally, there would be more than one perfectly calibrated transformer for both voltages and currents as multiple calibration processes could be performed for an overall better estimate. As for the line parameters estimation, at the end of 20 iterations, the difference between the true and estimated values of susceptance was in the order of 10e-6, and for impedance it was in the order of 10e-5.

Chapter 5: Conclusion and Future Work

5.1 Conclusions

With an increasing number of grid operators around the world deploying synchrophasors on their systems, maximum utility is naturally sought from these devices. While traditional problems like state estimation, frequency monitoring, post-mortem analysis might take the forefront during initial deployment stages, deeper dispersion of the technology will certainly result in increased significance of other applications such as transducer calibration and line parameter estimation. When instrument transformers do not operate within the error limits specified by the IEEE or IEC standards, they can cause significant miscalculations for downstream operations. Their calibration therefore not only improves accuracies of state estimation, load dispatch, revenue calculations at tie-lines, but can also help gauge the ages of different transformers. Over time this information can studied and used to decide when to upgrade necessary devices. When it comes to transmission line parameters, these are traditionally calculated through software. These depend on the length, cross-sectional area of the conductor, temperature and tower and conductor geometry. Seasonal or daily variations in temperature can also affect sag, which in turn would affect the parameters. Taking all these features into account for calculations renders it tricky to constantly track changes in parameters. However with the availability of real-time synchrophasor data, the parameters can be computed in real-time as well.

The objective of this thesis was to propose an efficient method to solve the problem of instrument transformer calibration and transmission line parameter estimation. The calibration process requires accurate line parameter data, and similarly to estimate the line parameters, accurate values of voltage and current are required. The fact that both sets of quantities to begin with could be erroneous poses an interesting conundrum.

Through this thesis an iterative method has been proposed and implemented, that shows progressive improvements in the calibration and parameter estimation processes.

Existing methods of instrument transformer calibration were discussed. The method was implemented on test cases using simulated synchrophasor measurements, assuming only one voltage measuring device had been perfectly calibrated. The results show how the errors in estimating the true values of voltage increase as we move further away from the perfect PT. The errors in estimation of currents were slightly higher than the voltage errors, but remained within an acceptable range. It is probable that the introduction of a perfectly calibrated CT would increase the accuracy of the calibration process.

Contemporary methods of line parameter estimation were also reviewed. A method employing the Kalman filter was then implemented to estimate the line parameters. An interesting outcome of this implementation was the difference in way the estimator worked for datasets having vast and gradual load shifts. Vast changes in voltages would imply that the samples had been taken at different times of the day. However, temperature changes along the day affect the line parameters. With this consideration, samples from a fixed span of time need to be considered, where the temperature remains relatively constant. Therefore a solution that utilized the currents was developed to employ the Kalman filter successfully.

Finally, the calibration process and the parameter estimation process were run successively and iteratively. The results showed a decrease in the errors of calibration over progressive iterations. The final difference between the true parameters and estimated parameters also remained within a small range.

5.2 Future Work

Although this thesis has proposed a method that shows promising results, there is certainly room to develop it further. At the time of this implementation, sufficient synchrophasor data was not available. A connected tree of measurements, which is required for the calibration process was also not found due to possible device

communication issues. In the future, a greater volume of data along with a connected set of measurements could be beneficial for validating the algorithm, and making improvements as necessary.

In this work, the method has been tested on fairly small systems and was found to work well. When the system size was increased to about 10 buses, the errors in current transformer calibration (specifically, the maximum deviation from true and calibrated values) were found to be slightly higher. As it is, in this work a perfectly calibrated current transformer was not considered. The inclusion of this could potentially increase the system size that could be calibrated via this method. Multiple perfectly calibrated instruments placed strategically across a large network would be the best case scenario, as each measurement would then be calibrated by more than one device, averaging out any errors.

Another topic that could be investigated is the PMU device error itself. The IEEE C37.118.1a-2014 is the current active standard for synchrophasor measurements on power systems. The standard defines acceptable error limits for PMUs in terms of Total Vector Error (TVE) which accounts for magnitude and angle, as well as Frequency Error and Rate of Change of Frequency Error. For most testing scenarios, the acceptable TVE limit is <1%. For devices operating outside these limits, the device error could propagate and result in incorrect calibration. It would be worthwhile for utilities to ensure that their PMUs are routinely calibrated.

References

[1] G. MISSOUT and P. Girard, "Measurement of Bus Voltage Angle Between Montreal and SEPT-ILES," *IEEE Transactions on Power Apparatus and Systems*, vol. PAS-99, pp. 536 - 539, 1980.

[2] P. Bonanomi, "Phase Angle Measurements with Synchronized Clocks – Principle and Applications," *IEEE Power Engineering Review*, vol. PER-1, pp. 50-50, 1981.

[3] G. Missout, J. Beland, G. Bedard, and Y. Lafleur, "Dynamic Measurement of the Absolute Voltage Angle on Long Transmission Lines," *IEEE Power Engineering Review*, vol. PER-1, pp. 23-24, 1981.

[4] A. G. Phadke, J. S. Thorp, and M. G. Adamiak, "A New Measurement Technique for Tracking Voltage Phasors, Local System Frequency, and Rate of Change of Frequency," *IEEE Power Engineering Review*, vol. PER-1, pp. 23-23, 1983.

[5] A. G. Phadke and J. S. Thorp, *Synchronized Phasor Measurements and Their Applications*: Springer US, 2008.

[6] "Macrodyne Model 1690 PMU Disturbance Recorder," ed.

[7] R. O. Burnett, M. M. Butts, T. W. Cease, V. Centeno, G. Michel, R. J. Murphy, *et al.*, "Synchronized Phasor Measurements of a Power System Event," *IEEE Transactions on Power Systems*, vol. 9, pp. 1643 - 1650, 1994.

[8] Z. Zhong, C. Xu, B. J. Billian, L. Zhang, S.-J. S. Tsai, R. W. Conners, *et al.*, "Power System Frequency Monitoring Network (FNET) Implementation," *IEEE Transactions on Power Systems*, vol. 20, pp. 1914 - 1921, 2005.

[9] D. Hu and V. M. Venkatasubramanian, "New Wide-Area Algorithms for Detection and Mitigation of Angle Instability using Synchrophasors," in *Power Engineering Society General Meeting*, 2007.

[10] IEEE, "C57.13-2008 - IEEE Standard Requirements for Instrument Transformers," ed, 2008, pp. c1 - 82.

[11] N. L. Kusters and W. J. M. Moore, "The Compensated Current Comparator; A New Reference Standard for Current-Transformer Calibrations in Industry," *IEEE Transactions on Instrumentation and Measurement*, vol. 13, pp. 107 - 114, 1964.

[12] I. Zoltan, "A New Self-Calibrating Instrument for Voltage Transformer Calibration," presented at the Conference on Precision Electromagnetic Measurements Digest, 1996.

[13] A. Brandolini, M. Faifer, and R. Ottoboni, "A Novel and Simple Method for VT and CT Calibration," presented at the Instrumentation and Measurement Technology Conference, 2008.

[14] A. Brandolini, M. Faifer, and R. Ottoboni, "A Simple Method for the Calibration of Traditional and Electronic Measurement Current and Voltage Transformers," *IEEE Transactions on Instrumentation and Measurement*, vol. 58, pp. 1345 - 1353, 2009.

[15] J. C. Santos, A. C. d. Sillos, and C. G. S. Nascimento, "On-field instrument transformers calibration using optical current and voltage transformes," presented

at the IEEE International Workshop on Applied Measurements for Power Systems Proceedings (AMPS) 2014.
[16] A. Pal, P. Chatterjee, J. S. Thorp, and V. A. Centeno, "Online Calibration of Voltage Transformers Using Synchrophasor Measurements," *IEEE Transactions on Power Delivery*, vol. 31, pp. 370 - 380, 2016.
[17] Z. Wu, K. Thomas, R. Sun, V. A. Centeno, and A. G. Phadke, "Three-phase instrument transformer calibration with synchronized phasor measurements," presented at the 2012 IEEE PES Innovative Smart Grid Technologies (ISGT), Washington, DC, 2012.
[18] Z. Wu, "Synchronized Phasor Measurement Units Applications in Three-phase Power System," Ph.D Dissertation, Electrical and Computer Engineering, Virginia Polytechnic Institute and State University, Blacksburg, VA, USA, 2013.
[19] K. R. Davis, S. Dutta, T. J. Overbye, and J. Gronquist, "Estimation of Transmission Line Parameters from Historical Data," presented at the 46th Hawaii International Conference on System Sciences (HICSS), 2013.
[20] R. E. Wilson, G. A. Zevenbergen, D. L. Mah, and A. J. Murphy, "Calculation of Transmission Line Parameters From Synchronized Measurements," *Electric Machines and Power Systems*, vol. 27, pp. 1269-1278, 1999.
[21] D. Shi, D. J. Tylavsky, N. Logic, and K. M. Koellner, "Identification of Short Transmission-Line Parameters from Synchrophasor Measurements," presented at the NAPS '08. 40th North American Power Symposium, 2008.
[22] M. Asprou and E. Kyriakides, "Estimation of Transmission Line Parameters Using PMU Measurements," presented at the IEEE Power & Energy Society General Meeting, 2015.
[23] C. Borda, A. Olarte, and H. Diaz, "PMU-based Line and Transformer Parameter Estimation," presented at the Power Systems Conference and Exposition, 2009.
[24] ABB, "Instrument Transformers Application Guide," ABB, Ed., ed.
[25] D. Dua, S. Dambhare, and R. K. Gajbhiye, "Optimal Multistage Scheduling of PMU Placement: An ILP Approach," *IEEE Transactions on Power Delivery*, vol. 23, pp. 1812 - 1820, 2008.
[26] G. Welch and G. Bishop, "An Introduction to the Kalman Filter."
[27] C. Mishra, V. A. Centeno, and A. Pal, "Kalman-filter based recursive regression for three-phase line parameter estimation using synchrophasor measurements," presented at the Power & Energy Society General Meeting, 2015 IEEE.

Appendix

Appendix A: Development of the covariance matrix R

Let us assume the errors in measurements belong to a normal distribution with mean 0. Let the voltage errors have a variance of σ_v^2 and the currents have a variance of σ_c^2. Now in equation (3.25), R is the covariance of the errors v_{sus}. A detailed explanation can be found in [27]. To compute the R matrix for susceptances, let b_n represent the n^{th}element of B_{sus}. The elements of the symmetric matrix R_{sus} can be computed from the equations (3.19) and (3.21) as below:

$$R_{sus}(1,1) = \sigma_v^2 * [(b_2 + b_4 + b_6)^2 + (b_7 + b_{10} + b_{12})^2 + b_4^2 + b_6^2 + b_{10}^2 + b_{12}^2] + 2\sigma_c^2 \quad \text{(A1)}$$

$$R_{sus}(2,2) = \sigma_v^2 * [(b_2 + b_4 + b_5)^2 + (b_8 + b_{10} + b_{11})^2 + b_4^2 + b_5^2 + b_{10}^2 + b_{11}^2] + 2\sigma_c^2 \quad \text{(A2)}$$

$$R_{sus}(3,3) = \sigma_v^2 * [(b_3 + b_5 + b_6)^2 + (b_9 + b_{11} + b_{12})^2 + b_5^2 + b_6^2 + b_{11}^2 + b_{12}^2] + 2\sigma_c^2 \quad \text{(A3)}$$

$$R_{sus}(1,2) = \sigma_v^2 * [-(b_1 + b_4 + b_6)b_4 - (b_2 + b_4 + b_5)b_4 + b_5 b_6 - (b_7 + b_{10} + b_{12})b_{10} - (b_8 + b_{10} + b_{11})b_{10} + b_{11} b_{12}] \quad \text{(A4)}$$

$$R_{sus}(1,3) = \sigma_v^2 * [-(b_1 + b_4 + b_6)b_4 - (b_5 + b_3 + b_6)b_6 + b_4 b_5 - (b_7 + b_{10} + b_{12})b_{12} - (b_{11} + b_9 + b_{12})b_{12} + b_{10} b_{11}] \quad \text{(A5)}$$

$$R_{sus}(2,3) = \sigma_v^2 * [-(b_2 + b_4 + b_5)b_5 - (b_3 + b_5 + b_6)b_5 + b_4 b_6 - (b_8 + b_{10} + b_{11})b_{11} - (b_9 + b_{11} + b_{12})b_{11} + b_{10} b_{12}] \quad \text{(A6)}$$

Similarly, for impedances, let us use equations (3.29) and (3.31) to obtain the elements of the error covariance matrix R. Let z_n represent the n_{th} element of Z_{imp}. The elements of R_{imp} then are:

$$R_{imp}(1,1) = \sigma_c^2 * [z_1^2 + z_4^2 + z_6^2 + z_7^2 + z_{10}^2 + z_{12}^2] - \sigma_v^2([z_1, z_4, z_6] * B_{p0}^{abc} * B_{p0}^{abcT} * [z_1, z_4, z_6]^T + [z_7 + 1, z_{10}, z_{12}] * B_{p0}^{abc} * B_{p0}^{abcT} * [z_7 + 1, z_{10}, z_{12}]^T) + \sigma_v^2 \quad \text{(A7)}$$

$$R_{imp}(2,2) = \sigma_c^2 * [z_4^2 + z_2^2 + z_5^2 + z_8^2 + z_{10}^2 + z_{11}^2] - \sigma_v^2([z_4, z_2, z_5] * B_{p0}^{abc} * B_{p0}^{abcT} * [z_4, z_2, z_5]^T + [z_{10}, z_8 + 1, z_{11}] * B_{p0}^{abc} * B_{p0}^{abcT} * [z_{10}, z_8 + 1, z_{11}]^T) + \sigma_v^2 \quad \text{(A8)}$$

$$R_{imp}(3,3) = \sigma_c^2 * [z_6^2 + z_5^2 + z_3^2 + z_{12}^2 + z_{11}^2 + z_9^2] - \sigma_v^2([z_6, z_5, z_3] * B_{p0}^{abc} * B_{p0}^{abcT} * [z_6, z_5, z_3]^T + [z_{12}, z_{11}, z_9 + 1] * B_{p0}^{abc} * B_{p0}^{abcT} * [z_{12}, z_{11}, z_9 + 1]^T) + \sigma_v^2 \quad \text{(A9)}$$

$$R_{imp}(1,2) = \sigma_c^2 * ([z_1, z_4, z_6, z_7, z_{10}, z_{12}] * [z_4, z_2, z_5, z_{10}, z_8, z_{11}]^T) - \sigma_v^2 * ([z_1, z_4, z_6] * B_{p0}^{abc} * B_{p0}^{abcT} * [z_4, z_2, z_5]^T + [z_7 + 1, z_{10}, z_{12}] * B_{p0}^{abc} * B_{p0}^{abcT} * [z_{10}, z_8 + 1, z_{11}]^T) \quad \text{(A10)}$$

$$R_{imp}(1,3) = \sigma_c^2 * ([z_1, z_4, z_6, z_7, z_{10}, z_{12}] * [z_6, z_5, z_3, z_{12}, z_{11}, z_9]^T) - \sigma_v^2 * ([z_1, z_4, z_6] * B_{p0}^{abc} * B_{p0}^{abcT} * [z_6, z_5, z_3]^T + [z_7 + 1, z_{10}, z_{12}] * B_{p0}^{abc} * B_{p0}^{abcT} * [z_{12}, z_{11}, z_9 + 1]^T) \quad \text{(A11)}$$

$$R_{imp}(2,3) = \sigma_c^2 * ([z_1, z_4, z_6, z_7, z_{10}, z_{12}] * [z_6, z_5, z_3, z_{12}, z_{11}, z_9]^T) - \sigma_v^2 * ([z_1, z_4, z_6] * B_{p0}^{abc} * B_{p0}^{abcT} * [z_6, z_5, z_3]^T + [z_7 + 1, z_{10}, z_{12}] * B_{p0}^{abc} * B_{p0}^{abcT} * [z_{12}, z_{11}, z_9 + 1]^T) \quad \text{(A12)}$$

$$R_{imp}(1,4) = \sigma_c^2 * ([z_1, z_4, z_6, z_7, z_{10}, z_{12}] * [z_7, z_{10}, z_{12}, -z_1, -z_4, -z_6]^T) - \sigma_v^2 * ([z_1, z_4, z_6] * B_{p0}^{abc} * B_{p0}^{abcT} * [z_7 + 1, z_{10}, z_{12}]^T - [z_7 + 1, z_{10}, z_{12}] * B_{p0}^{abc} * B_{p0}^{abcT} * [z_1, z_4, z_6]^T) \quad \text{(A13)}$$

$$R_{imp}(1,5) = \sigma_c^2 * ([z_1, z_4, z_6, z_7, z_{10}, z_{12}] * [z_{10}, z_8, z_{11}, -z_4, -z_2, -z_5]^T) - \sigma_v^2 * ([z_1, z_4, z_6] * B_{p0}^{abc} * B_{p0}^{abcT} * [z_{10}, z_8 + 1, z_{11}]^T - [z_7 + 1, z_{10}, z_{12}] * B_{p0}^{abc} * B_{p0}^{abcT} * [z_4, z_2, z_5]^T) \quad \text{(A14)}$$

$$R_{imp}(1,6) = \sigma_c^2 * ([z_1, z_4, z_6, z_7, z_{10}, z_{12}] * [z_{12}, z_{11}, z_9, -z_6, -z_5, -z_3]^T) - \sigma_v^2 * ([z_1, z_4, z_6] * B_{p0}^{abc} * B_{p0}^{abcT} * [z_{12}, z_{11}, z_9 + 1]^T - [z_7 + 1, z_{10}, z_{12}] * B_{p0}^{abc} * B_{p0}^{abcT} * [z_6, z_5, z_3]^T) \quad \text{(A15)}$$

$$R_{imp}(2,4) = \sigma_c^2 * ([z_4, z_2, z_5, z_{10}, z_8, z_{11}] * [z_7, z_{10}, z_{12}, -z_4, z_2, z_5]^T) - \sigma_v^2 * ([z_4, z_2, z_5] * B_{p0}^{abc} * B_{p0}^{abcT} * [z_7 + 1, z_{10}, z_{12}]^T - [z_{10}, z_8 + 1, z_{11}] * B_{p0}^{abc} * B_{p0}^{abcT} * [z_1, z_4, z_6]^T) \quad \text{(A16)}$$

$$R_{imp}(2,5) = \sigma_c^2 * ([z_4, z_2, z_5, z_{10}, z_8, z_{11}] * [z_{10}, z_8, z_{11}, -z_4, -z_2, -z_5]^T) - \sigma_v^2 * ([z_4, z_2, z_5] * B_{p0}^{abc} * B_{p0}^{abcT} * [z_{10}, z_8 + 1, z_{11}]^T - [z_{10}, z_8 + 1, z_{11}] * B_{p0}^{abc} * B_{p0}^{abcT} * [z_4, z_2, z_5]^T) \quad \text{(A17)}$$

$$R_{imp}(2,6) = \sigma_c^2 * ([z_4, z_2, z_5, z_{10}, z_8, z_{11}] * [z_{12}, z_{11}, z_9, -z_6, -z_5, -z_3]^T) - \sigma_v^2 * ([z_4, z_2, z_5] * B_{p0}^{abc} * B_{p0}^{abcT} * [z_{12}, z_{11}, z_9 + 1]^T - [z_{10}, z_8 + 1, z_{11}] * B_{p0}^{abc} * B_{p0}^{abcT} * [z_6, z_5, z_3]^T) \quad \text{(A18)}$$

$$R_{imp}(3,4) = \sigma_c^2 * ([z_6, z_5, z_3, z_{12}, z_{11}, z_9] * [z_7, z_{10}, z_{12}, -z_4, z_2, z_5]^T) - \sigma_v^2 * ([z_6, z_5, z_3] * B_{p0}^{abc} * B_{p0}^{abcT} * [z_7 + 1, z_{10}, z_{12}]^T - [z_{12}, z_{11}, z_9 + 1] * B_{p0}^{abc} * B_{p0}^{abcT} * [z_1, z_4, z_6]^T) \quad \text{(A19)}$$

$$R_{imp}(3,5) = \sigma_c^2 * ([z_6, z_5, z_3, z_{12}, z_{11}, z_9] * [z_{10}, z_8, z_{11}, -z_4, -z_2, -z_5]^T) - \sigma_v^2 * ([z_6, z_5, z_3] * B_{p0}^{abc} * B_{p0}^{abcT} * [z_{10}, z_8 + 1, z_{11}]^T - [z_{12}, z_{11}, z_9 + 1] * B_{p0}^{abc} * B_{p0}^{abcT} * [z_4, z_2, z_5]^T) \quad \text{(A20)}$$

$$R_{imp}(3,6) = \sigma_c^2 * ([z_6, z_5, z_3, z_{12}, z_{11}, z_9] * [z_{12}, z_{11}, z_9, -z_6, -z_5, -z_3]^T) - \sigma_v^2 * ([z_6, z_5, z_3] * B_{p0}^{abc} * B_{p0}^{abcT} * [z_{12}, z_{11}, z_9 + 1]^T - [z_{12}, z_{11}, z_9 + 1] * B_{p0}^{abc} * B_{p0}^{abcT} * [z_6, z_5, z_3]^T) \quad \text{(A21)}$$

This matrix is symmetric and can be built with the elements described above.

Appendix B: Features of MATLAB Code

MATLAB Code: Calibration function

```
function [V_cal,Ipq_cal, Iqp_cal, CFPTmag, CFPTangd, CFCTmag,
CFCTangd,kk] = cal_piece(Vp,Vq,Ipq,Iqp,Z,B)
% Function to perform claibration line by line

num = length(Vp);

Y = inv(Z);
B = B./2;

AA = [];
BB = [];

for i = 1: num
    xa = [ Y*diag(Vq(:,i))                    diag(Ipq(:,i))
zeros(3,3);
           (-Y*diag(Vq(:,i))-B*diag(Vq(:,i)))     zeros(3,3)       -
diag(Iqp(:,i))];

    AA = [AA; xa];


    xb = [ (Y+B)*(Vp(:,i));
           -Y*(Vp(:,i)) ];

    BB = [BB; xb];
end
xx = [real(AA)      -imag(AA);
      imag(AA)      real(AA) ];

yy = [real(BB); imag(BB)];

xhat = xx\yy;


kk = complex(xhat(1:9), xhat(10:18));

for i = 1:num
V_cal(:,i) = Vq(:,i).* kk(1:3);
Ipq_cal(:,i) = Ipq(:,i).*kk(4:6);
Iqp_cal(:,i) = Ipq(:,i).*kk(7:9);
end

CFPTmag = abs(kk(1:3));
CFPTangd = rad2deg(angle(kk(1:3)));
CFCTmag = abs(kk(4:9));
CFCTangd = rad2deg(angle(kk(4:9)));
```

MATLAB Code: Calibration on a Two Bus System

```
% Calling the calibration function for a given two bus system dataset
% Outputs Calibrated values and Correction Factors
% cal_piece_2_bus.m

clc;
clear all;
close all;

% Load dataset of V,I
load dGH_vi_act_20

num = length(Vpa);

%*********************************************************************%
% Original values of Z & B
load zb_GH
%*********************************************************************%
% Generate errors
a = 1;
b = 10e-3;
ang = 0.05;

for j = 1:3
        errv1(j,1) = 1;
        errv2(j,1) = (a + b*randn)*exp((1i*ang*randn)*pi/180);
        errc1(j,1) = (a + b*randn)*exp((1i*ang*randn)*pi/180);
        errc2(j,1) = (a + b*randn)*exp((1i*ang*randn)*pi/180);
end

errv = [errv1; errv2];
errc = [errc1; errc2];

for i = 1:num
    Vp(:,i) = Vpa(:,i).*errv1;
    Vq(:,i) = Vqa(:,i).*errv2;
    Ipq(:,i) = Ipqa(:,i).*errc1;
    Iqp(:,i) = -Iqpa(:,i).*errc2;
end

%*********************************************************************%

[V_cal,Ipq_cal, Iqp_cal, CFPTmag, CFPTangd, CFCTmag, CFCTangd,kk] =
cal_piece(Vp,Vq,Ipq,Iqp,Z_orig,B_orig);

% Computing errors in correction factors
errPTmag= abs(errv(4:end,:).^(-1)) - CFPTmag;
errPTangd = rad2deg(angle(errv(4:end).^(-1))) - CFPTangd;

errCTmag = abs(errc(:,:).^(-1)) - CFCTmag;
errCTangd = rad2deg(angle(errc.^(-1))) - CFCTangd;
```

```
end
```

MATLAB Code: Kalman Filter Line Parameter Estimation on a Two Bus System

```
% Kalman Filter Line Parameter Estimation - Largely Fluctuating Data
% Results for T
% Code for A
% 23 Dec 2016

clc;
clear all;
close all;

%%%*****************************************************************
**************
% Generate Data
Vpa_mag_a = [1   1.05    0.95    0.97    1.01    1.03    1.1     1.02
0.99    0.96    0.97    0.98    1.03    1.02    0.99    0.975   1.015
0.995   1.0     1.02   ];
Vpa_mag = [Vpa_mag_a;Vpa_mag_a;Vpa_mag_a];


Vqa_mag_a = [ 0.9500  1.0000  0.90    1.01    1.02    1.05    0.97
0.90    0.92    0.99    0.97    1.02    1.01    0.98    0.96    1.0
0.98    0.99    1   0.9     ];
Vqa_mag = [Vqa_mag_a;Vqa_mag_a;Vqa_mag_a];

Vpa_ang = [ 0   -90     45      45      30      0       90      22.5
-45     -90     30  120     120     -22.5     36      18      -180    -
45     90      120 ;
            30  120     120     -22.5     36      18      -180    -45
90      120   -90 -30     90      90      60      120     -90     180
-90     60;
            -90 -30     90      90      60      120     -90     180
-90     60      0   -90     45      45      30      0       90
22.5    -45     -90 ];

Vqa_ang = [ 0       -90     45      22.5    -45     120     60      18
180     0          -180    60      -90     45      -90     0       30
25.7143     180     120;
            30      120     120     90      -15     -120    -22.5   -30
120     -180        30      120     120     90      -15     -120    -
22.5   -30     120     -180;
            -180    60      -90     45      -90     0       30
25.7143     180     120     0       -90     45      22.5    -45     120
60      18      180     0];

Vpa = complex(Vpa_mag.*cosd(Vpa_ang), Vpa_mag.*sind(Vpa_ang));
Vqa = complex(Vqa_mag.*cosd(Vqa_ang), Vqa_mag.*sind(Vqa_ang));


Ba = 3; Bb = 4; Bc = 5; Bab = 2; Bbc = 2; Bca = 2;
```

```
B = 1i*[ Ba+Bab+Bca      -Bab        -Bca;
         -Bab          Bb+Bab+Bbc    -Bbc;
         -Bca            -Bbc      Bc+Bbc+Bca ];

Z = [ 3+4i    2i    2i;
       2i    4+5i   2i;
       2i     2i   3+2i ];

Ipqa = inv(Z) * (Vpa - Vqa) + B*Vpa;
Iqpa = inv(Z) * (Vqa - Vpa) + B*Vqa;


% Vpa = Vpa(:,1:10);
% Vqa = Vqa(:,1:10);
% Ipqa = Ipqa(:,1:10);
% Iqpa = Iqpa(:,1:10);
%%%*************************************************************************
**************
%%%*************************************************************************
**************


load err_klpe;
errv1 = errv(1:3,:);
errv2 = errv(4:6,:);
errc1 = errc(1:3,:);
errc2 = errc(4:6,:);
for i = 1:num
    Vp(:,i) = Vpa(:,i).*errv1;
    Vq(:,i) = Vqa(:,i).*errv2;
    Ipq(:,i) = Ipqa(:,i).*errc1;
    Iqp(:,i) = Iqpa(:,i).*errc2;
end


% Vp = Vpa;
% Vq = Vqa;
% Ipq = Ipqa;
% Iqp = Iqpa;
% %
% sigv = 10e-8;
% sigc = 10e-9;
% [Bp,Xp,tol_bb, tol_xx] = est(Vp,Vq,Ipq,Iqp,Z,B,sigv,sigc );


sigv = 10e-4;
sigc = 10e-3;

for i = 1:1
%%%*************************************************************************
**************
% Begin Estimation of Suscepatances
CaseNum = length(Iqpa);
% % To use values without error
```

```
% Ipq = Ipqa;%(:,1:20);
% Iqp = Iqpa;%(:,1:20);
% Vp = Vpa;%(:,1:20);
% Vq = Vqa;%(:,1:20);

% sigv = 10e-9;
% sigc = 10e-9;
% sigv = 10e-5;
% sigc = 10e-7;

theta_sus = zeros(12,1);
P_sus = eye(12,12);
% CaseNum = 20;
for k = 1:CaseNum

    theta_init = theta_sus(:,k); % unused

    zsh = Ipq(:,k) + Iqp(:,k);

    Hsh = [ Vp(1,k)      0        0        Vp(1,k)-Vp(2,k)      0
Vp(1,k)-Vp(3,k)      Vq(1,k)      0        0        Vq(1,k)-Vq(2,k)      0
Vq(1,k)-Vq(3,k);
            0          Vp(2,k)    0        Vp(2,k)-Vp(1,k) Vp(2,k)-Vp(3,k)
0                    0      Vq(2,k)    0        Vq(2,k)-Vq(1,k)  Vq(2,k)-
Vq(3,k)         0           ;
            0            0      Vp(3,k)        0            Vp(3,k)-Vp(2,k)
Vp(3,k)-Vp(1,k)          0        0        Vq(3,k)      0
Vq(3,k)-Vq(2,k)     Vq(3,k)-Vq(1,k)];

   zsus = [ real(zsh); imag(zsh)];

   Hsus = [ -imag(Hsh); real(Hsh)];

   % Calculation of Rnew
   R11 = sigv^2 * ((theta_sus(1)+theta_sus(4)+theta_sus(6))^2 +
(theta_sus(7)+theta_sus(10)+theta_sus(12))^2 + (theta_sus(4))^2 +
(theta_sus(6))^2 + (theta_sus(10))^2 + (theta_sus(12))^2) +2*sigc^2;

   R22 = sigv^2 * ((theta_sus(2)+theta_sus(4)+theta_sus(5))^2 +
(theta_sus(8)+theta_sus(10)+theta_sus(11))^2 + (theta_sus(4))^2 +
(theta_sus(5))^2 + (theta_sus(10))^2 + (theta_sus(11))^2) +2*sigc^2;

   R33 = sigv^2 * ((theta_sus(3)+theta_sus(5)+theta_sus(6))^2 +
(theta_sus(9)+theta_sus(11)+theta_sus(12))^2 + (theta_sus(5))^2 +
(theta_sus(6))^2 + (theta_sus(11))^2 + (theta_sus(12))^2) +2*sigc^2;

   R12 = sigv^2 * (-
(theta_sus(1)+theta_sus(4)+theta_sus(6))*theta_sus(4) -
(theta_sus(2)+theta_sus(4)+theta_sus(5))*theta_sus(4) +
theta_sus(5)*theta_sus(6) -
(theta_sus(7)+theta_sus(10)+theta_sus(12))*theta_sus(10) -
(theta_sus(8)+theta_sus(10)+theta_sus(11))*theta_sus(10) +
theta_sus(11)*theta_sus(12));
```

```
   R13 = sigv^2 * (-
(theta_sus(1)+theta_sus(4)+theta_sus(6))*theta_sus(6) -
(theta_sus(5)+theta_sus(3)+theta_sus(6))*theta_sus(6) +
theta_sus(4)*theta_sus(5) -
(theta_sus(7)+theta_sus(10)+theta_sus(12))*theta_sus(12) -
(theta_sus(11)+theta_sus(9)+theta_sus(12))*theta_sus(12) +
theta_sus(10)*theta_sus(11));

   R23 = sigv^2 * (-
(theta_sus(2)+theta_sus(4)+theta_sus(5))*theta_sus(5) -
(theta_sus(3)+theta_sus(5)+theta_sus(6))*theta_sus(5) +
theta_sus(4)*theta_sus(6) -
(theta_sus(8)+theta_sus(10)+theta_sus(11))*theta_sus(11) -
(theta_sus(9)+theta_sus(11)+theta_sus(12))*theta_sus(11) +
theta_sus(10)*theta_sus(12));

   R = [ R11    R12     R13;
         R12    R22     R23;
         R13    R23     R33 ];

   Rnew = [R  zeros(3,3);zeros(3,3)  R];
%    Rnew = zeros(6,6);
   K = P_sus * Hsus.'/(Hsus * P_sus * Hsus.' + Rnew);

   theta_sus(:,k+1) = theta_sus(:,k) + K*(zsus - Hsus*theta_sus(:,k));
%    theta_sus = theta_sus + K*(zsus - Hsus*theta_sus);

   P_sus = eye(12) - K*Hsus*P_sus;

    variation (:,k) = theta_sus(:,k+1) - theta_init;  % unused

    tol_b1(k) = theta_sus(1,k+1) - theta_sus(1,k);
    tol_b2(k) = theta_sus(2,k+1) - theta_sus(2,k);
    tol_b3(k) = theta_sus(3,k+1) - theta_sus(3,k);
    tol_b4(k) = theta_sus(4,k+1) - theta_sus(4,k);
    tol_b5(k) = theta_sus(5,k+1) - theta_sus(5,k);
    tol_b6(k) = theta_sus(6,k+1) - theta_sus(6,k);
end

clear K;
clear R11;clear R12;clear R13;clear R22;clear R23;clear R33;
% Form susceptance matrices from values obtained
bp_an = theta_sus(1,end);
bp_bn = theta_sus(2,end);
bp_cn = theta_sus(3,end);
bp_abn = theta_sus(4,end);
bp_bcn = theta_sus(5,end);
bp_can = theta_sus(6,end);

bq_an = theta_sus(7,end);
bq_bn = theta_sus(8,end);
bq_cn = theta_sus(9,end);
bq_abn = theta_sus(10,end);
bq_bcn = theta_sus(11,end);
```

```
bq_can = theta_sus(12,end);

Bp = 1i*[ bp_an+bp_abn+bp_can          -bp_abn         -bp_can;
                -bp_abn         bp_bn+bp_abn+bp_bcn     -bp_bcn;
                -bp_can                 -bp_bcn     bp_cn+bp_bcn+bp_can
];

Bq =  1i*[ bq_an+bq_abn+bq_can          -bq_abn         -bq_can;
                -bq_abn         bq_bn+bq_abn+bq_bcn     -bq_bcn;
                -bq_can                 -bq_bcn     bq_cn+bq_bcn+bq_can
];


% Begin Estimation of Impedances
theta_imp = ones(12,1);
P_imp = eye(12,12);
% Bp = B;
% sigv = 10e-4;
% sigc = 10e-3;
for k = 1: CaseNum
    zse = Vp(:,k) - Vq(:,k);

    h1 = Ipq(1,k) - [Bp(1,1)    Bp(1,2)     Bp(1,3)]*Vp(:,k);
    h2 = Ipq(2,k) - [Bp(2,1)    Bp(2,2)     Bp(2,3)]*Vp(:,k);
    h3 = Ipq(3,k) - [Bp(3,1)    Bp(3,2)     Bp(3,3)]*Vp(:,k);

    hh(:,k) = Ipq(:,k) - Bp*Vp(:,k);

    Hse = [ h1  0   0   h2  0   h3;
            0   h2  0   h1  h3  0;
            0   0   h3  0   h2  h1 ];

    zimp = [ real(zse); imag(zse)];

    Himp = [ real(Hse)   -imag(Hse);
             imag(Hse)    real(Hse) ];

    % Calculation of Rnew
    R11 = sigc^2 * ((theta_imp(1))^2 + (theta_imp(4))^2 +
(theta_imp(6))^2 + (theta_imp(7))^2 + (theta_imp(10))^2 +
(theta_imp(12))^2) - sigv^2 *
([theta_imp(1),theta_imp(4),theta_imp(6)]*Bp*Bp.'*[theta_imp(1),theta_i
mp(4),theta_imp(6)].' +
[theta_imp(7)+1,theta_imp(10),theta_imp(12)]*Bp*Bp.'*[theta_imp(7)+1,th
eta_imp(10),theta_imp(12)].') + sigv^2;

    R22 = sigc^2 * ((theta_imp(4))^2 + (theta_imp(2))^2 +
(theta_imp(5))^2 + (theta_imp(10))^2 + (theta_imp(8))^2 +
(theta_imp(11))^2) - sigv^2 *
([theta_imp(4),theta_imp(2),theta_imp(5)]*Bp*Bp.'*[theta_imp(4),theta_i
mp(2),theta_imp(5)].' +
[theta_imp(10),theta_imp(8)+1,theta_imp(11)]*Bp*Bp.'*[theta_imp(10),the
ta_imp(8)+1,theta_imp(11)].') + sigv^2;
```

```
    R33 = sigc^2 * ((theta_imp(6))^2 + (theta_imp(5))^2 +
(theta_imp(3))^2 + (theta_imp(12))^2 + (theta_imp(11))^2 +
(theta_imp(9))^2) - sigv^2 *
([theta_imp(6),theta_imp(5),theta_imp(3)]*Bp*Bp.'*[theta_imp(6),theta_i
mp(5),theta_imp(3)].' +
[theta_imp(12),theta_imp(11),theta_imp(9)+1]*Bp*Bp.'*[theta_imp(12),the
ta_imp(11),theta_imp(9)+1].') + sigv^2;

    R12 = sigc^2 *
([theta_imp(1),theta_imp(4),theta_imp(6),theta_imp(7),theta_imp(10),the
ta_imp(12)]*[theta_imp(4),theta_imp(2),theta_imp(5),theta_imp(10),theta
_imp(8),theta_imp(11)].') -
sigv^2*([theta_imp(1),theta_imp(4),theta_imp(6)]*Bp*Bp.'*[theta_imp(4),
theta_imp(2),theta_imp(5)].' +
[theta_imp(7)+1,theta_imp(10),theta_imp(12)]*Bp*Bp.'*[theta_imp(10),the
ta_imp(8)+1,theta_imp(11)].');

    R13 = sigc^2 *
([theta_imp(1),theta_imp(4),theta_imp(6),theta_imp(7),theta_imp(10),the
ta_imp(12)]*[theta_imp(6),theta_imp(5),theta_imp(3),theta_imp(12),theta
_imp(11),theta_imp(9)].') -
sigv^2*([theta_imp(1),theta_imp(4),theta_imp(6)]*Bp*Bp.'*[theta_imp(6),
theta_imp(5),theta_imp(3)].' +
[theta_imp(7)+1,theta_imp(10),theta_imp(12)]*Bp*Bp.'*[theta_imp(12),the
ta_imp(11),theta_imp(9)+1].');

    R23 = sigc^2 *
([theta_imp(4),theta_imp(2),theta_imp(5),theta_imp(10),theta_imp(8),the
ta_imp(11)]*[theta_imp(6),theta_imp(5),theta_imp(3),theta_imp(12),theta
_imp(11),theta_imp(9)].') -
sigv^2*([theta_imp(4),theta_imp(2),theta_imp(5)]*Bp*Bp.'*[theta_imp(6),
theta_imp(5),theta_imp(3)].' +
[theta_imp(10),theta_imp(8)+1,theta_imp(11)]*Bp*Bp.'*[theta_imp(12),the
ta_imp(11),theta_imp(9)+1].');

    R14 = sigc^2 *
([theta_imp(1),theta_imp(4),theta_imp(6),theta_imp(7),theta_imp(10),the
ta_imp(12)]*[theta_imp(7),theta_imp(10),theta_imp(12),-theta_imp(1),-
theta_imp(4),-theta_imp(6)].') -
sigv^2*([theta_imp(1),theta_imp(4),theta_imp(6)]*Bp*Bp.'*[theta_imp(7)+
1,theta_imp(10),theta_imp(12)].' -
[theta_imp(7)+1,theta_imp(10),theta_imp(12)]*Bp*Bp.'*[theta_imp(1),thet
a_imp(4),theta_imp(6)].');

    R15 = sigc^2 *
([theta_imp(1),theta_imp(4),theta_imp(6),theta_imp(7),theta_imp(10),the
ta_imp(12)]*[theta_imp(10),theta_imp(8),theta_imp(11),-theta_imp(4),-
theta_imp(2),-theta_imp(5)].') -
sigv^2*([theta_imp(1),theta_imp(4),theta_imp(6)]*Bp*Bp.'*[theta_imp(10)
,theta_imp(8)+1,theta_imp(11)].' -
[theta_imp(7)+1,theta_imp(10),theta_imp(12)]*Bp*Bp.'*[theta_imp(4),thet
a_imp(2),theta_imp(5)].');

    R16 = sigc^2 *
([theta_imp(1),theta_imp(4),theta_imp(6),theta_imp(7),theta_imp(10),the
```

```
ta_imp(12)]*[theta_imp(12),theta_imp(11),theta_imp(9),-theta_imp(6),-
theta_imp(5),-theta_imp(3)].') -
sigv^2*([theta_imp(1),theta_imp(4),theta_imp(6)]*Bp*Bp.'*[theta_imp(12)
,theta_imp(11),theta_imp(9)+1].' -
[theta_imp(7)+1,theta_imp(10),theta_imp(12)]*Bp*Bp.'*[theta_imp(6),thet
a_imp(5),theta_imp(3)].');

    R24 = sigc^2 *
([theta_imp(4),theta_imp(2),theta_imp(5),theta_imp(10),theta_imp(8),the
ta_imp(11)]*[theta_imp(7),theta_imp(10),theta_imp(12),-
theta_imp(4),theta_imp(2),theta_imp(5)].') -
sigv^2*([theta_imp(4),theta_imp(2),theta_imp(5)]*Bp*Bp.'*[theta_imp(7)+
1,theta_imp(10),theta_imp(12)].' -
[theta_imp(10),theta_imp(8)+1,theta_imp(11)]*Bp*Bp.'*[theta_imp(1),thet
a_imp(4),theta_imp(6)].');

    R25 = sigc^2 *
([theta_imp(4),theta_imp(2),theta_imp(5),theta_imp(10),theta_imp(8),the
ta_imp(11)]*[theta_imp(10),theta_imp(8),theta_imp(11),-theta_imp(4),-
theta_imp(2),-theta_imp(5)].') -
sigv^2*([theta_imp(4),theta_imp(2),theta_imp(5)]*Bp*Bp.'*[theta_imp(10)
,theta_imp(8)+1,theta_imp(11)].' -
[theta_imp(10),theta_imp(8)+1,theta_imp(11)]*Bp*Bp.'*[theta_imp(4),thet
a_imp(2),theta_imp(5)].');

    R26 = sigc^2 *
([theta_imp(4),theta_imp(2),theta_imp(5),theta_imp(10),theta_imp(8),the
ta_imp(11)]*[theta_imp(12),theta_imp(11),theta_imp(9),-theta_imp(6),-
theta_imp(5),-theta_imp(3)].') -
sigv^2*([theta_imp(4),theta_imp(2),theta_imp(5)]*Bp*Bp.'*[theta_imp(12)
,theta_imp(11),theta_imp(9)+1].' -
[theta_imp(10),theta_imp(8)+1,theta_imp(11)]*Bp*Bp.'*[theta_imp(6),thet
a_imp(5),theta_imp(3)].');

    R34 = sigc^2 *
([theta_imp(6),theta_imp(5),theta_imp(3),theta_imp(12),theta_imp(11),th
eta_imp(9)]*[theta_imp(7),theta_imp(10),theta_imp(12),-
theta_imp(4),theta_imp(2),theta_imp(5)].') -
sigv^2*([theta_imp(6),theta_imp(5),theta_imp(3)]*Bp*Bp.'*[theta_imp(7)+
1,theta_imp(10),theta_imp(12)].' -
[theta_imp(12),theta_imp(11),theta_imp(9)+1]*Bp*Bp.'*[theta_imp(1),thet
a_imp(4),theta_imp(6)].');

    R35 = sigc^2 *
([theta_imp(6),theta_imp(5),theta_imp(3),theta_imp(12),theta_imp(11),th
eta_imp(9)]*[theta_imp(10),theta_imp(8),theta_imp(11),-theta_imp(4),-
theta_imp(2),-theta_imp(5)].') -
sigv^2*([theta_imp(6),theta_imp(5),theta_imp(3)]*Bp*Bp.'*[theta_imp(10)
,theta_imp(8)+1,theta_imp(11)].' -
[theta_imp(12),theta_imp(11),theta_imp(9)+1]*Bp*Bp.'*[theta_imp(4),thet
a_imp(2),theta_imp(5)].');

    R36 = sigc^2 *
([theta_imp(6),theta_imp(5),theta_imp(3),theta_imp(12),theta_imp(11),th
eta_imp(9)]*[theta_imp(12),theta_imp(11),theta_imp(9),-theta_imp(6),-
```

```
theta_imp(5),-theta_imp(3)].') -
sigv^2*([theta_imp(6),theta_imp(5),theta_imp(3)]*Bp*Bp.'*[theta_imp(12)
,theta_imp(11),theta_imp(9)+1].' -
[theta_imp(12),theta_imp(11),theta_imp(9)+1]*Bp*Bp.'*[theta_imp(6),thet
a_imp(5),theta_imp(3)].');


    Rnew2 = [   R11    R12     R13     R14     R15     R16;
                R12    R22     R23     R24     R25     R26;
                R13    R23     R33     R34     R35     R36;
                R14    R24     R34     R11     R12     R13;
                R15    R25     R35     R12     R22     R23;
                R16    R26     R36     R13     R23     R33 ];

   K = P_imp * Himp.'/(Himp * P_imp * Himp.' + Rnew2);

   theta_imp(:,k+1) = theta_imp(:,k) + K*(zimp - Himp*theta_imp(:,k));
%    theta_imp = theta_imp + K*(zimp - Himp*theta_imp);

   P_imp = eye(12) - K*Himp*P_imp;

%     variation (:,k) = theta_sus(:,k+1) - theta_init;

    tol_x1(k) = theta_imp(1,k+1) - theta_imp(1,k);
    tol_x2(k) = theta_imp(2,k+1) - theta_imp(2,k);
    tol_x3(k) = theta_imp(3,k+1) - theta_imp(3,k);
    tol_x4(k) = theta_imp(4,k+1) - theta_imp(4,k);
    tol_x5(k) = theta_imp(5,k+1) - theta_imp(5,k);
    tol_x6(k) = theta_imp(6,k+1) - theta_imp(6,k);

end
xp_an = theta_imp(1,end) + 1i* theta_imp(7,end);
xp_bn = theta_imp(2,end) + 1i* theta_imp(8,end);
xp_cn = theta_imp(3,end) + 1i* theta_imp(9,end);
xp_abn = theta_imp(4,end)+ 1i* theta_imp(10,end);
xp_bcn = theta_imp(5,end)+ 1i* theta_imp(11,end);
xp_can = theta_imp(6,end)+ 1i* theta_imp(12,end);

Xp = [ xp_an    xp_abn  xp_can;
       xp_abn   xp_bn   xp_bcn;
       xp_can   xp_bcn  xp_cn ];



figure(1)
plot(tol_b1,'r')
hold on
plot(tol_b2,'b')
hold on
plot(tol_b3,'g')
hold on
plot(tol_b4,'-y')
hold on
plot(tol_b5,'-m')
```

```
hold on
plot(tol_b6,'-c')
xlabel('Iteration number','FontSize',25)
ylabel('Difference between succesive estimates','FontSize',25)
title('Tolerances of Susceptances','FontSize',30)
legend('Baa','Bbb','Bcc','Bab','Bbc','Bca')
set(gcf,'color','w');
set(gca,'fontsize',20)


figure(2)
plot(tol_x1,'r')
hold on
plot(tol_x2,'b')
hold on
plot(tol_x3,'g')
hold on
plot(tol_x4,'-y')
hold on
plot(tol_x5,'-m')
hold on
plot(tol_x6,'-c')
xlabel('Iteration number','FontSize',25)
ylabel('Difference between succesive estimates','FontSize',25)
title('Tolerances of Impedances','FontSize',30)
legend('Xa','Xb','Xc','Xab','Xbc','Xca')
set(gcf,'color','w');
set(gca,'fontsize',20)


end


B
Bp
Z
Xp

B-Bp
Z-Xp
```

MATLAB Code: Iterative Method

```
% Iteration
% Two Bus Sim Data
% Results for T
% Code for A
% 5 Jan 2017

% dataset dGH_vi_act/_20 are from simulated load scaling

clc;
clear all;
close all;


% Load dataset of V,I
load dGH_vi_act_20

num = length(Vpa);
V_act = [Vpa;Vqa];
I_act = [Ipqa;Iqpa];

%*************************************************************************
*************%
% Original values
for i = 1:1
Z_orig =[   0.0014647+0.01409i    0.0011683+0.0071112i
0.0011637+0.0073451i;
        0.0011683+0.0071112i    0.0014747+0.014062i
0.001168+0.0066315i;
        0.0011637+0.0073451i    0.001168+0.0066315i
0.0014653+0.014102i ];

B_orig =[   0.53705i     -0.08962i  -0.102425i ;
        -0.08962i   +0.531625i  -0.0505175i;
        -0.102425i  -0.0505175i +0.536675i ];
end
%*************************************************************************
*************%
%*************************************************************************
*************%
% Generate errors
a = 1;
b = 10e-2;
ang = 0.05;

for j = 1:3
        errv1(j,1) = 1;
        errv2(j,1) = (a + b*randn)*exp((1i*ang*randn)*pi/180);
        errc1(j,1) = (a + b*randn)*exp((1i*ang*randn)*pi/180);
        errc2(j,1) = (a + b*randn)*exp((1i*ang*randn)*pi/180);
end
```

```
errv = [errv1; errv2];
errc = [errc1; errc2];


% Errors on Z & B
errb = 0.1*randn(3,3)+ones(3,3);
errz = 0.1*randn(3,3) + ones(3,3);

% Apply errors to V, I, Z, B
for i = 1:num
    V_mea(:,i) = V_act(:,i).*errv;
    I_mea(:,i) = I_act(:,i).*errc;
end
B_mea = B_orig.*errb;
Z_mea = Z_orig.*errz;
%**************************************************************************
************%
%**************************************************************************
************%

% Number of lines
nl = 1;

V_cal = {};
I_cal = {};
ZZ = {};
BB = {};

for k = 1:10

    if k ==1
        VV_cal = [V_act(1:3,:)];
        Ipq_cal = [];
        Iqp_cal = [];

        for m = 1:nl

%             if m ==1
                Vp = V_mea(m*3-2:m*3,:);
                Vq = V_mea(3*m-2+3:3*m+3,:);
                Ipq = I_mea(3*m-2:3*m,:);
                Iqp = -I_mea(3*m-2+3:3*m+3,:);

%             else
%                 Vp = VV_cal(m*3-2:m*3,:);
%                 Vq = V_mea(3*m-2+3:3*m+3,:);
%                 Ipq = I_mea(3*m-2:3*m,:);
%                 Iqp = -I_mea(3*m+13:3*m+15,:);
%             end

            Z = Z_mea(:,m*3-2:m*3);
            B = B_mea(:,m*3-2:m*3);
```

```
            [V_cal2,Ipq_cal2, Iqp_cal2, CFPTmagx, CFPTangdx, CFCTmagx,
CFCTangdx,kk] = cal_piece(Vp,Vq,Ipq,Iqp,Z,B);

            CFPTmag(3*m-2:3*m,1) = CFPTmagx;
            CFPTangd(3*m-2:3*m,1) = CFPTangdx;
            CFCTmag(6*m-5:6*m,1) = CFCTmagx;
            CFCTangd(6*m-5:6*m,1) = CFCTangdx;

            VV_cal = [VV_cal; V_cal2];
            Ipq_cal = [Ipq_cal ; Ipq_cal2];
            Iqp_cal = [Iqp_cal; -Iqp_cal2];

            CFPT(3*m-2:3*m,1) = kk(1:3,1);
            CFCT(6*m-5:6*m,1) = kk(4:9,1);

        end
        % Computing errors in correction factors
    errPTmag= abs(errv(4:end,:).^(-1)) - CFPTmag;
    errPTangd = rad2deg(angle(errv(4:end).^(-1))) - CFPTangd;

    errCTmag = abs(errc(:,:).^(-1)) - CFCTmag;
    errCTangd = rad2deg(angle(errc.^(-1))) - CFCTangd;



    % Calibrated values
    VV_cal = VV_cal;
    II_cal = [Ipq_cal;Iqp_cal];
    V_cal{1,k} = VV_cal;
    I_cal{1,k} = II_cal;

    % Line Parameter Estimation
    for m = 1:nl
        Vp = VV_cal(m*3-2:m*3,:);
        Vq = VV_cal(3*m-2+3:3*m+3,:);
        Ipq = II_cal(3*m-2:3*m,:);
        Iqp = II_cal(3*m-2+3:3*m+3,:);

        %********** Calculate voltages from currents
        Z = Z_orig(:,m*3-2:m*3);
        B = B_orig(:,m*3-2:m*3);
        W = Z*B;

        X = [ (eye(3)+W)    -eye(3);
              -eye(3,3)  (eye(3)+W) ];

        num = length(Ipq);

        for i = 1:num
            Y = [ Z*Ipq(:,i);
                 Z*Iqp(:,i) ];

            Vx(:,i) = inv(X) * Y;
```

```
        end
        %**********
        Vp2 = Vx(1:3,:);
        Vq2 = Vx(4:6,:);
        Ipq2 = Ipq;
        Iqp2 = Iqp;

        sigv = 10e-7; sigc = 10e-9;


        [Bp,Xp,tol_bb, tol_xx] = est(Vp2,Vq2,Ipq2,Iqp2,Z,B,sigv,sigc );
        close all;

        ZZ{1,k}(:,m*3-2:m*3) = Xp;
        BB{1,k}(:,m*3-2:m*3) =  Bp;
    end




elseif k>1
            VV_cal = [V_act(1:3,:)];
            Ipq_cal = [];
            Iqp_cal = [];
            for m = 1:nl
%             if m ==1
                Vp = V_mea(m*3-2:m*3,:);
                Vq = V_cal{1,k-1}(3*m-2+3:3*m+3,:);
                Ipq = I_cal{1,k-1}(3*m-2:3*m,:);
                Iqp = -I_cal{1,k-1}(3*m-2+3:3*m+3,:);

%             else
%                 Vp = VV_cal(m*3-2:m*3,:);
%                 Vq = V_cal{1,k-1}(3*m-2+3:3*m+3,:);
%                 Ipq = I_cal{1,k-1}(3*m-2:3*m,:);
%                 Iqp = -I_cal{1,k-1}(3*m-2+3:3*m+3,:);
%             end

            Z = ZZ{1,k-1}(:,m*3-2:m*3);
            B = BB{1,k-1}(:,m*3-2:m*3);

            [V_cal2,Ipq_cal2, Iqp_cal2, CFPTmagx, CFPTangdx, CFCTmagx,
CFCTangdx,kk] = cal_piece(Vp,Vq,Ipq,Iqp,Z,B);

            CFPTmag(3*m-2:3*m,1) = CFPTmagx;
            CFPTangd(3*m-2:3*m,1) = CFPTangdx;
            CFCTmag(6*m-5:6*m,1) = CFCTmagx;
            CFCTangd(6*m-5:6*m,1) = CFCTangdx;

            VV_cal = [VV_cal; V_cal2];
            Ipq_cal = [Ipq_cal ; Ipq_cal2];
```

```
        Iqp_cal = [Iqp_cal; -Iqp_cal2];

        CFPT(3*m-2:3*m,1) = kk(1:3,1);
        CFCT(6*m-5:6*m,1) = kk(4:9,1);

    end
    % Computing errors in correction factors
errPTmag= abs(errv(4:end,:).^(-1)) - CFPTmag;
errPTangd = rad2deg(angle(errv(4:end).^(-1))) - CFPTangd;

errCTmag = abs(errc(:,:).^(-1)) - CFCTmag;
errCTangd = rad2deg(angle(errc.^(-1))) - CFCTangd;


% Calibrated values
VV_cal = VV_cal;
II_cal = [Ipq_cal;Iqp_cal];
V_cal{1,k} = VV_cal;
I_cal{1,k} = II_cal;

% Line Parameter Estimation
for m = 1:nl
    Vp = VV_cal(m*3-2:m*3,:);
    Vq = VV_cal(3*m-2+3:3*m+3,:);
    Ipq = II_cal(3*m-2:3*m,:);
    Iqp = II_cal(3*m-2+3:3*m+3,:);

    %********** Calculate voltages from currents
    Z = Z_orig(:,m*3-2:m*3);
    B = B_orig(:,m*3-2:m*3);
    W = Z*B;

    X = [ (eye(3)+W)    -eye(3);
          -eye(3,3)  (eye(3)+W) ];

    num = length(Ipq);

    for i = 1:num
        Y = [ Z*Ipq(:,i);
             Z*Iqp(:,i) ];

        Vx(:,i) = inv(X) * Y;

    end
    %**********
    Vp2 = Vx(1:3,:);
    Vq2 = Vx(4:6,:);
    Ipq2 = Ipq;
    Iqp2 = Iqp;

    sigv = 10e-7; sigc = 10e-8;
```

```
        [Bp,Xp,tol_bb, tol_xx] = est(Vp2,Vq2,Ipq2,Iqp2,Z,B,sigv,sigc );
         close all;
        ZZ{1,k}(:,m*3-2:m*3) = Xp;
        BB{1,k}(:,m*3-2:m*3) =  Bp;
    end


    end

  disp(sprintf('End of Round %g', k));
(B_orig-BB{1,k}).'
(Z_orig-ZZ{1,k}).'


%     V_cal{1,k} = VV_cal;
%     I_cal{1,k} = [Ipq_cal;Iqp_cal];
%



end
for i = 1:k
    vdiff(:,i) = mean(mean(V_act-V_cal{1,i}));
    idiff(:,i) = mean(mean(I_act-I_cal{1,i}));
    vmaxd(:,i) = max(max(V_act-V_cal{1,i}));
    imaxd(:,i) = max(max(I_act-I_cal{1,i}));

end
% Capture differences for each phase
for i = 1:k
    xxv = V_act-V_cal{1,i};
    xxi = I_act-I_cal{1,i};

    vda(:,i) = mean(xxv(1:3:end,:).');
    vdb(:,i) = mean(xxv(2:3:end,:).');
    vdc(:,i) = mean(xxv(3:3:end,:).');

    ida(:,i) = mean(xxi(1:3:end,:).');
    idb(:,i) = mean(xxi(2:3:end,:).');
    idc(:,i) = mean(xxi(3:3:end,:).');

    vdam(:,i) = max(xxv(1:3:end,:).');
    vdbm(:,i) = max(xxv(2:3:end,:).');
    vdcm(:,i) = max(xxv(3:3:end,:).');

    idam(:,i) = max(xxi(1:3:end,:).');
    idbm(:,i) = max(xxi(2:3:end,:).');
    idcm(:,i) = max(xxi(3:3:end,:).');

end

figure()
% subplot(2,1,1)
```

```
surf(abs(vda.'),'FaceColor','blue')
hold on
surf(abs(vdb.'),'FaceColor','green')
hold on
surf(abs(vdc.'),'FaceColor','yellow')
ylabel('No of iterations', 'FontSize',25)
zlabel('Deviation in p.u.', 'FontSize',25)
xlabel('Bus Number', 'FontSize',25)
legend('Phase A','Phase B','Phase C')
title('Voltages: Average Difference btwn Real & Calibrated Values',
'FontSize',30)
set(gca,'fontsize',20)

% subplot(2,1,2)
figure()
surf(abs(ida.'),'FaceColor','blue')
hold on
surf(abs(idb.'),'FaceColor','green')
hold on
surf(abs(idc.'),'FaceColor','yellow')
ylabel('No of iterations', 'FontSize',25)
zlabel('Deviation in p.u.', 'FontSize',25)
xlabel('Branch Number', 'FontSize',25)
legend('Phase A','Phase B','Phase C')
title('Currents (Ipq,Iqp): Average Difference btwn Real & Calibrated
Values', 'FontSize',30)
% [ax,h]=subtitle('Average Difference btwn Real & Calibrated Values');
set(gca,'fontsize',20)




figure()
% subplot(2,1,1)
plot(abs(vdiff));
xlabel('No. of iterations', 'FontSize',25)
ylabel('Deviation in p.u.', 'FontSize',25)
title('Voltages: Average Difference btwn Real & Calibrated Values',
'FontSize',30)
set(gca,'fontsize',20)

% subplot(2,1,2)
figure()
plot(abs(idiff));
xlabel('No. of iterations', 'FontSize',25)
ylabel('Deviation in p.u.', 'FontSize',25)
title('Currents: Average Difference btwn Real & Calibrated Values',
'FontSize',30)
set(gca,'fontsize',20)

figure()
% subplot(2,1,1)
plot(abs(vmaxd));
xlabel('No. of iterations', 'FontSize',25)
ylabel('Deviation in p.u.', 'FontSize',25)
```

```
title('Voltages : Maximum Difference btwn Real & Calibrated Values',
'FontSize',30)
set(gca,'fontsize',20)

figure()
% subplot(2,1,2)
plot(abs(imaxd));
xlabel('No. of iterations', 'FontSize',25)
ylabel('Deviation in p.u.', 'FontSize',25)
title('Currents: Maximum Difference btwn Real & Calibrated Values',
'FontSize',30)
set(gca,'fontsize',20)
```